Search for supersymmetry in events with *b*-quark jets and missing transverse energy in *pp* collisions at 7 TeV

S. Chatrchyan *et al.**

(CMS Collaboration)

Results are presented from a search for physics beyond the standard model based on events with large missing transverse energy, at least three jets, and at least one, two, or three *b*-quark jets. The study is performed using a sample of proton-proton collision data collected at $\sqrt{s} = 7$ TeV with the CMS detector at the LHC in 2011. The integrated luminosity of the sample is 4.98 fb^{-1}. The observed number of events is found to be consistent with the standard model expectation, which is evaluated using control samples in the data. The results are used to constrain cross sections for the production of supersymmetric particles decaying to *b*-quark-enriched final states in the context of simplified model spectra.

I. INTRODUCTION

Many extensions of the standard model (SM) predict that events in high-energy proton-proton collisions can contain large missing transverse energy ($E_{\mathrm{T}}^{\mathrm{miss}}$) and multiple, high-transverse momentum (p_{T}) jets. For example, in *R*-parity-conserving [1] models of supersymmetry (SUSY) [2], SUSY particles are created in pairs. Each member of the pair initiates a decay chain that terminates with the lightest SUSY particle (LSP) and SM particles. If the LSP only interacts weakly, as in the case of a dark-matter candidate, it escapes detection, potentially yielding significant $E_{\mathrm{T}}^{\mathrm{miss}}$. Furthermore, in some scenarios [3], the SUSY partners of the bottom and top quarks can be relatively light, leading to the enhanced production of events with bottom-quark jets (*b* jets). Events of this type, with *b* jets and large $E_{\mathrm{T}}^{\mathrm{miss}}$, represent a distinctive topological signature that is the subject of a search described in this paper.

We present a search for new physics (NP) in events with large $E_{\mathrm{T}}^{\mathrm{miss}}$, no isolated leptons, three or more high-p_{T} jets, and at least one, two, or three *b* jets. The analysis is based on a sample of proton-proton collision data collected at $\sqrt{s} = 7$ TeV with the Compact Muon Solenoid (CMS) detector at the CERN Large Hadron Collider (LHC) in 2011, corresponding to an integrated luminosity of 4.98 fb^{-1}. Recent searches for NP in a similar final state are presented in Refs. [4–8]. Our analysis is characterized by a strong reliance on techniques that use control samples in data to evaluate the SM background.

The principal sources of the SM background are events with top quarks, comprising $t\bar{t}$-pair and single-top-quark events, events with a *W* or *Z* boson accompanied by jets,

and nontop multijet events produced purely through strong-interaction processes. We hereafter refer to this last class of events as "QCD" background. Diboson (*WW*, *ZZ*, or *WZ*) events represent a smaller source of background. For events with a *W* boson or a top quark, significant $E_{\mathrm{T}}^{\mathrm{miss}}$ can arise if a *W* boson decays into a charged lepton and a neutrino. The neutrino provides a source of genuine $E_{\mathrm{T}}^{\mathrm{miss}}$. Similarly, significant $E_{\mathrm{T}}^{\mathrm{miss}}$ can arise in events with a *Z* boson if the *Z* boson decays to two neutrinos. For QCD-background events, significant $E_{\mathrm{T}}^{\mathrm{miss}}$ arises primarily from the mismeasurement of jet p_{T}. A smaller component of the QCD background arises from events with semileptonic decays of *b* and *c* quarks.

We interpret our results in the context of simplified model spectra (SMS) [9–12], which provide a general framework to characterize NP signatures. They include only a few NP particles and focus on generic topologies. We consider the SMS scenarios denoted T1bbbb and T1tttt. Event diagrams are shown in Fig. 1. These two models are characterized by *b*-jet-enriched final states, large jet multiplicities, and large $E_{\mathrm{T}}^{\mathrm{miss}}$ values, making our analysis sensitive to their production. For convenience, we express SMS phenomenology using SUSY nomenclature. In T1bbbb (T1tttt), pair-produced gluinos $\tilde{g}$ each decay into two *b*-quark jets (*t*-quark jets) and the LSP, taken to be the lightest neutralino $\tilde{\chi}^0$. The LSP is assumed to escape detection, leading to significant $E_{\mathrm{T}}^{\mathrm{miss}}$. If the SUSY partner of the bottom quark (top quark) is much lighter than any other squark, with the gluino yet lighter, gluino decays are expected to be dominated by the three-body process shown in Figs. 1(a) and 1(b).

As benchmark NP scenarios, we choose the T1bbbb and T1tttt models with gluino mass $m_{\tilde{g}} = 925$ GeV and LSP mass $m_{\mathrm{LSP}} = 100$ GeV, with normalization to the next-to-leading order (NLO) plus next-to-leading-logarithm (NLL) cross section [13–17]. These two benchmark models lie near the boundary of our expected sensitivity.

In Secs. II and III we describe the detector and event selection. Section IV introduces the $\Delta\hat{\phi}_{\mathrm{min}}$ variable, used in the evaluation of the QCD background. Our techniques

---

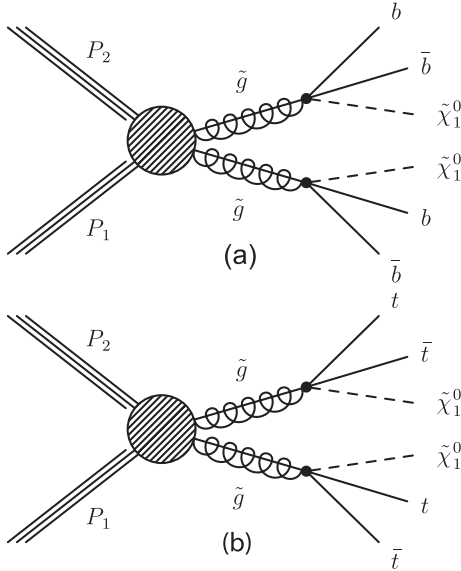*Full author list given at the end of the article.

FIG. 1. Event diagrams for the (a) T1bbbb and (b) T1tttt simplified models.

to evaluate the SM background from control samples in data are presented in Sec. V. In Sec. VI we describe our analysis framework, based on a likelihood method that simultaneously determines the SM background and tests the consistency of NP models with the data, taking into account possible NP contamination of control sample regions. The interpretation of our results is presented in Sec. VII. A summary of the analysis is given in Sec. VIII.

II. DETECTOR AND TRIGGER

A detailed description of the CMS detector is given elsewhere [18]. The CMS coordinate system is defined with the origin at the center of the detector and the z axis along the direction of the counterclockwise beam. The transverse plane is perpendicular to the beam axis, with ϕ the azimuthal angle (measured in radians), θ the polar angle, and $\eta = -\ln[\tan(\theta/2)]$ the pseudorapidity. A superconducting solenoid provides an axial magnetic field of 3.8 T. Within the field volume are a silicon pixel and strip tracker, a crystal electromagnetic calorimeter, and a brass-scintillator hadron calorimeter. Muons are detected with gas-ionization chambers embedded in the steel flux-return yoke outside the solenoid. The tracker covers the region $|\eta| < 2.5$ and the calorimeters $|\eta| < 3.0$. The region $3 < |\eta| < 5$ is instrumented with a forward calorimeter. The near-hermeticity of the detector permits accurate measurements of energy balance in the transverse plane.

The principal trigger used for the analysis selects events based on the quantities H_T and H_T^{miss}, where H_T is the scalar sum of the transverse energy of jets and H_T^{miss} the modulus of the corresponding vector sum. Because of increasing beam collision rates, trigger conditions vary over the period of data collection. The most stringent trigger requirements are $H_T >$

350 GeV and $H_T^{\text{miss}} > 110$ GeV. The efficiency of the H_T component for the final event selection is measured from data to be 86% (99%) for H_T values of 400 GeV (500 GeV). The efficiency of the H_T^{miss} component is 98% for $E_T^{\text{miss}} > 250$ GeV. Appropriate corrections are applied to account for trigger inefficiencies and uncertainties in the various control and search regions of the analysis.

III. EVENT SELECTION

Physics objects are defined using the particle flow (PF) method [19], which is used to reconstruct and identify charged and neutral hadrons, electrons (with associated bremsstrahlung photons), muons, tau leptons, and photons, using an optimized combination of information from CMS subdetectors. The PF objects serve as input for jet reconstruction, based on the anti-k_T algorithm [20] with distance parameter 0.5. Jet corrections [21] are applied to account for residual effects of nonuniform detector response in both p_T and η. The missing transverse energy E_T^{miss} is defined as the modulus of the vector sum of the transverse momenta of all PF objects. The E_T^{miss} vector is the negative of the same vector sum.

The basic event selection criteria are as follows:
(1) at least one well-defined primary event vertex [22];
(2) at least three jets with $p_T > 50$ GeV and $|\eta| < 2.4$;
(3) a lepton veto defined by requiring that there be no identified, isolated electron or muon candidate [23,24] with $p_T > 10$ GeV; electron candidates are restricted to $|\eta| < 2.5$ and muon candidates to $|\eta| < 2.4$;
(4) $\Delta\hat{\phi}_{\text{min}} > 4.0$, where the $\Delta\hat{\phi}_{\text{min}}$ variable is described in Sec. IV.

Electrons and muons are considered isolated if the scalar sum of the transverse momenta of charged hadrons, photons, and neutral hadrons surrounding the lepton within a cone of radius $\sqrt{(\Delta\eta)^2 + (\Delta\phi)^2} = 0.3$, divided by the lepton p_T value itself, is less than 0.20 for electrons and 0.15 for muons.

To identify b jets, we use the combined-secondary-vertex algorithm at the medium working point [25]. This algorithm combines information about secondary vertices, track impact parameters, and jet kinematics to separate b jets from light-flavored-quark, charm-quark, and gluon jets. To increase sensitivity to NP scenarios, which often predict soft b jets, we use all tagged b jets with $p_T > 30$ GeV. The nominal b-jet-tagging efficiency is about 75% for jets with a p_T value of 100 GeV, as determined from a sample of b-jet-enriched dijet events [25]. (For b jets with $p_T \approx 30$ GeV, this efficiency is about 60%.) The corresponding misidentification rate is about 1.0%. We correct the simulated efficiencies for b-jet tagging and misidentification to match the efficiencies measured with control samples in the data. The b-tagging correction factor depends slightly on the jet p_T and has a typical value of 0.95. The uncertainty on this correction factor varies from 0.03 to 0.07 for b jets with p_T

from 30 to 670 GeV, and is taken to be 0.13 for b jets with $p_T > 670$ GeV.

We define five signal regions, which partially overlap, to enhance sensitivity in different kinematic regimes. The five regions correspond to different minimum requirements on H_T, E_T^{miss}, and the number of b jets. H_T is calculated using jets with $p_T > 50$ GeV and $|\eta| < 2.4$. The five regions, denoted 1BL, 1BT, 2BL, 2BT, and 3B, are specified in Table I and have been chosen without considering the data to avoid possible bias. The regions are selected based on expected signal and background event yields in simulation, to provide maximal sensitivity for discovery of the NP scenarios considered in this paper or, in the case of non-discovery, to best set limits on their parameters. Throughout this paper, we use the generic designation "SIG" to refer to any or all of these five signal regions.

The distributions of the number of tagged b jets for the 1BL, 1BT, and 2BT samples (i.e., for the three different sets of selection criteria on H_T and E_T^{miss}), except without the requirement on the number of b jets, are shown in Fig. 2. The results are presented in comparison with Monte Carlo (MC) simulations of SM processes. Results from the benchmark T1bbbb and T1tttt NP models mentioned in Sec. I are also shown. The simulated $t\bar{t}$, W + jets, and Z + jets events are produced at the parton level with the MADGRAPH5.1.1.0 [26] event generator. Single-top-quark events are generated with the POWHEG301 [27] program. The PYTHIA6.4.22 program [28] is used to produce diboson and QCD events. For all simulated samples, PYTHIA6.4 is used to describe parton showering and hadronization. All samples are generated using the CTEQ6 [29] parton distribution functions. The description of the detector response is implemented using the GEANT4 [30] program. The $t\bar{t}$ sample is normalized to the measured cross section [31]. The other simulated samples are normalized using the most accurate cross-section calculations currently available, which is generally NLO. The jet energy resolution in the simulation is corrected to account for a small discrepancy with respect to data [21]. In addition, the simulated samples are reweighted to describe the probability distribution observed in data for overlapping pp collisions within a bunch crossing ("pileup").

TABLE I. The definition of the signal (SIG) regions. The minimum requirements on H_T, E_T^{miss}, and the number of tagged b jets N_{bjets} are given. The designations $1b$, $2b$, and $3b$ refer to the minimum N_{bjets} value, while "loose" and "tight" refer to less restrictive and more restrictive selection requirements, respectively, for H_T and E_T^{miss}.

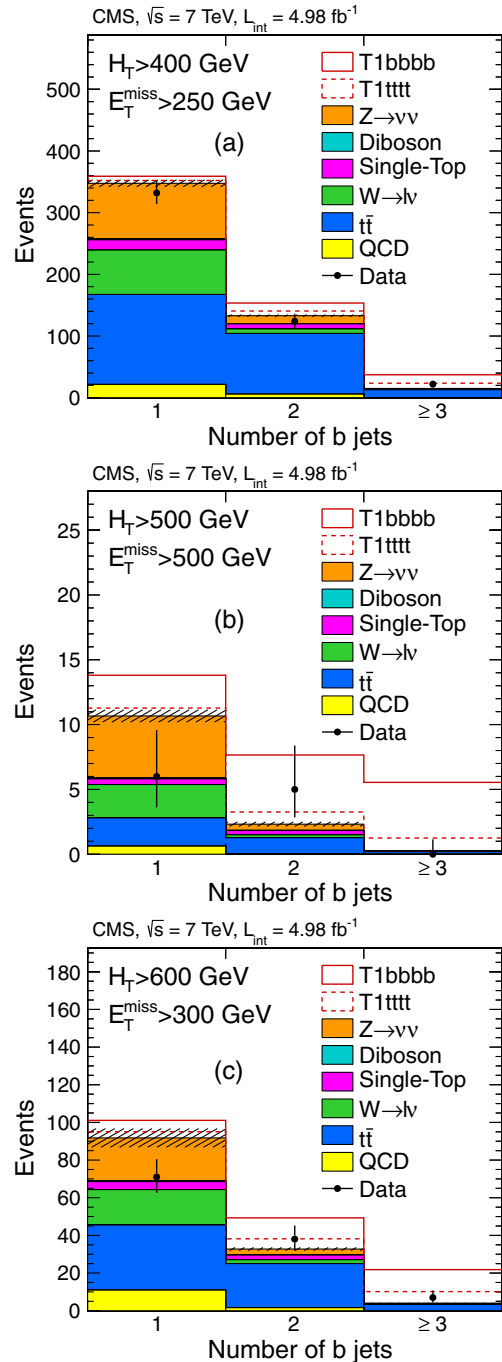| Signal region		H_T (GeV)	E_T^{miss} (GeV)	N_{bjets}
$1b$-loose	1BL	>400	>250	≥ 1
$1b$-tight	1BT	>500	>500	≥ 1
$2b$-loose	2BL	>400	>250	≥ 2
$2b$-tight	2BT	>600	>300	≥ 2
$3b$	3B	>400	>250	≥ 3

FIG. 2 (color online). The distributions of the number of tagged b jets for event samples selected with the (a) 1BL, (b) 1BT, and (c) 2BT requirements, except for the requirement on the number of b jets. The hatched bands show the statistical uncertainty on the total SM background prediction from simulation. The open histograms show the expectations for the T1bbbb (solid line) and T1tttt (dashed line) NP models, both with $m_{\tilde{g}} = 925$ GeV, $m_{LSP} = 100$ GeV, and normalization to NLO + NLL.

As examples illustrating the characteristics of events with at least one, two, or three tagged b jets, the E_T^{miss} distributions of events in the 1BL, 2BT, and 3B samples are shown in Fig. 3. The numbers of events in the different signal regions
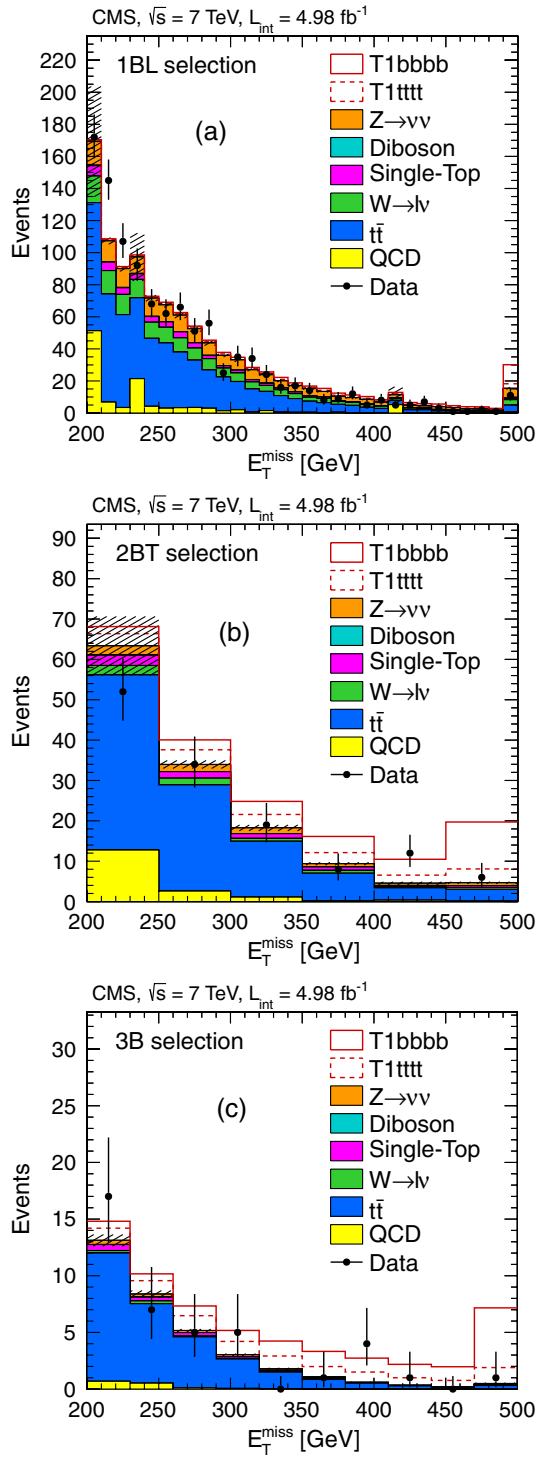
FIG. 3 (color online). The distributions of E_T^{miss} for event samples selected with the (a) 1BL, (b) 2BT, and (c) 3B requirements, except for the requirement on E_T^{miss}. The simulated spectra are normalized as in Fig. 2. The hatched bands show the statistical uncertainty on the total SM background prediction from simulation. The rightmost bin in all plots includes event overflow. The open histograms show the expectations for the T1bbbb (solid line) and T1tttt (dashed line) NP models, both with $m_{\tilde{g}} = 925$ GeV, $m_{LSP} = 100$ GeV, and normalization to NLO + NLL.

are listed in Table II for data and simulation. The simulated results are for guidance only and are not used in the analysis.

IV. THE $\Delta\hat{\phi}_{min}$ VARIABLE

Our method to evaluate the QCD background is based on the $\Delta\hat{\phi}_{min}$ variable. This method presumes that most E_T^{miss} in a QCD event arises from the p_T mismeasurement of a single jet.

The $\Delta\hat{\phi}_{min}$ variable is a modified version of the commonly used quantity $\Delta\phi_{min} \equiv \min(\Delta\phi_i)$ ($i = 1, 2, 3$), the minimum azimuthal opening angle between the E_T^{miss} vector and each of the three highest-p_T jets in an event. Misreconstruction of a jet primarily affects the modulus of its transverse momentum but not its direction. Thus QCD-background events are characterized by small values of $\Delta\phi_{min}$. The $\Delta\phi_{min}$ variable is strongly correlated with E_T^{miss}, as discussed below. This correlation undermines its utility for the evaluation of the QCD background from data. To reduce this correlation, we divide the $\Delta\phi_i$ by their estimated resolutions $\sigma_{\Delta\phi,i}$ to obtain $\Delta\hat{\phi}_{min} \equiv \min(\Delta\phi_i/\sigma_{\Delta\phi,i})$.

The resolution $\sigma_{\Delta\phi,i}$ for jet i is evaluated by considering the p_T resolution σ_{p_T} of the other jets in the event. The uncertainty σ_{T_i} on the component of the E_T^{miss} vector perpendicular to jet i is found using $\sigma_{T_i}^2 \equiv \sum_n (\sigma_{p_T,n} \sin\alpha_n)^2$, where the sum is over all other jets in the event with $p_T > 30$ GeV and α_n is the angle between jet n and the direction opposite jet i. The situation is depicted in Fig. 4 for an event with exactly three jets with $p_T > 30$ GeV. Our estimate of the $\Delta\phi$ resolution is $\sigma_{\Delta\phi,i} = \arctan(\sigma_{T_i}/E_T^{miss})$. [Note: $\arcsin(\sigma_{T_i}/E_T^{miss})$ is technically more correct in this expression; we use $\arctan(\sigma_{T_i}/E_T^{miss})$ because it is computationally more robust while being equivalent for the small angles of interest here.] For the jet p_T resolution, it suffices to use the simple linear parametrization $\sigma_{p_T} = 0.10 p_T$ [21].

Figure 5(a) shows the ratio of the number of events with $\Delta\phi_{min} > 0.3$ to the number with $\Delta\phi_{min} < 0.3$ as a function of E_T^{miss}, for a simulated QCD sample selected with the 1 BL requirements except for those on $\Delta\hat{\phi}_{min}$ and E_T^{miss}. ($\Delta\phi_{min} > 0.3$ or a similar criterion is commonly used to reject QCD background; see, e.g., Refs. [5–8].) The strong correlation between $\Delta\phi_{min}$ and E_T^{miss} is evident. The corresponding result based on $\Delta\hat{\phi}_{min}$ is shown in Fig. 5(b). For the latter figure we choose $\Delta\hat{\phi}_{min} = 4.0$ in place of $\Delta\phi_{min} = 0.3$, which yields a similar selection efficiency. For values of E_T^{miss} greater than about 30 GeV, the distribution based on $\Delta\hat{\phi}_{min}$ is seen to be far less dependent on E_T^{miss} than that based on $\Delta\phi_{min}$. Figure 5(c) shows the result corresponding to Fig. 5(b) for events with zero tagged b jets. Comparing Figs. 5(b) and 5(c), it is seen that the ratio $N(\Delta\hat{\phi}_{min} \geq 4.0)/N(\Delta\hat{\phi}_{min} < 4.0)$ has an approximately constant value of about 0.13 (for $E_T^{miss} > 30$ GeV) irrespective of the number of b jets.

The measured results for $N(\Delta\hat{\phi}_{min} \geq 4.0)/N(\Delta\hat{\phi}_{min} < 4.0)$ with zero b jets, for events with $H_T > 400$ GeV,

TABLE II.   The number of data events and corresponding predictions from MC simulation for the signal regions, with normalization to 4.98 fb^{-1}. The uncertainties on the simulated results are statistical.

	1BL	1BT	2BL	2BT	3B
Data	478	11	146	45	22
Total SM MC	496 ± 7	13.3 ± 0.6	148 ± 2	36.8 ± 0.9	15.0 ± 0.2
$t\bar{t}$	257 ± 2	3.6 ± 0.2	111 ± 1	26.7 ± 0.4	12.6 ± 0.2
Single-top quark	26.0 ± 1.0	0.8 ± 0.2	9.1 ± 0.5	2.7 ± 0.3	0.88 ± 0.09
W + jets	80.0 ± 1.0	2.8 ± 0.2	7.7 ± 0.3	2.2 ± 0.2	0.38 ± 0.05
$Z \rightarrow \nu\bar{\nu}$	104 ± 2	5.3 ± 0.4	13.8 ± 0.7	3.5 ± 0.3	0.80 ± 0.10
Diboson	1.8 ± 0.1	0.10 ± 0.02	0.27 ± 0.04	0.05 ± 0.02	0.02 ± 0.01
QCD	28.0 ± 6.0	0.70 ± 0.20	6.0 ± 1.0	1.7 ± 0.6	0.29 ± 0.07

500 GeV, and 600 GeV, are shown in Fig. 6. By requiring that there not be a b jet, we reduce the contribution of top-quark events, which is helpful for the evaluation of QCD background (Sec. VA). The data in Fig. 6 are collected with a prescaled H_T trigger, allowing events to be selected at low E_T^{miss} without a trigger bias. The data in Fig. 6(a) are seen to somewhat exceed the simulated predictions. The trend is visible in Fig. 6(b) to a lesser extent. This modest discrepancy arises because the $\Delta\hat{\phi}_{min}$ distribution is narrower in the simulation than in data. Since our method to evaluate the QCD background is based on the measured distribution, this feature of the simulation does not affect our analysis. The data in Fig. 6 are seen to exhibit the general behavior expected from the simulation. The region below around 100 GeV is seen to be dominated by the QCD background.

V. BACKGROUND EVALUATION

In this section we describe our methods to evaluate the SM background from control samples in data. Each of the three main backgrounds—from QCD, Z + jets, and top-quark and W + jets events (where "top quark" includes both $t\bar{t}$ and single-top-quark events)—is evaluated separately. We group top-quark and W + jets events together
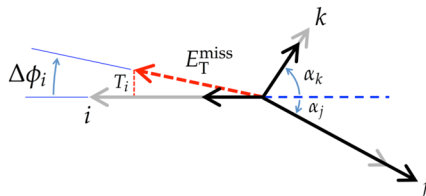

FIG. 4 (color online).   Illustration of variables used to calculate $\Delta\hat{\phi}_{min}$ for the case of an event with exactly three jets with $p_T >$ 30 GeV. The light-shaded (light gray) solid arrows show the true p_T values of the three jets i, j, and k. The dark-shaded (black) solid arrows show the reconstructed jet p_T values. The angles of jets j and k with respect to the direction opposite to jet i are denoted α_j and α_k. The E_T^{miss} for the event is shown by the dashed (red) arrow. The component of E_T^{miss} perpendicular to jet i, denoted T_i, is shown by the dotted vertical (red) line. σ_{T_i} is the uncertainty on T_i. $\Delta\phi_i$ is the angle between E_T^{miss} and jet i.

because they have a similar experimental signature. Note that our final results for the total SM background are derived from a global likelihood procedure that incorporates our background evaluation procedures into a single fit, and that also accounts for possible NP contributions to the control regions in a consistent manner. The global likelihood procedure is described in Sec. VI.

QCD background is evaluated using the $\Delta\hat{\phi}_{min}$ variable. Background from Z + jets events is evaluated by scaling the measured rates of $Z \rightarrow \ell^+\ell^-$ ($\ell = e$ or μ) events. To estimate the top-quark and W + jet background, we employ two complementary techniques. One, which we call the nominal method, is simple and almost entirely data based, while the other, which we call the E_T^{miss}-reweighting method, combines results based on data with information from simulation to examine individual sources of top-quark and W + jets background in detail.

A. QCD background

The low level of correlation between $\Delta\hat{\phi}_{min}$ and E_T^{miss} allows us to employ a simple method to evaluate the QCD background from data. As discussed in Sec. IV, the ratio $N(\Delta\hat{\phi}_{min} \geq 4.0)/N(\Delta\hat{\phi}_{min} < 4.0)$ is approximately independent of E_T^{miss}, and also of the number of b jets, for QCD events. Furthermore, the E_T^{miss} distribution below 100 GeV is expected to be dominated by QCD events, especially for events with zero b jets (Fig. 6). We therefore measure $N(\Delta\hat{\phi}_{min} \geq 4.0)/N(\Delta\hat{\phi}_{min} < 4.0)$ in a low E_T^{miss} region of the zero-b-jet sample and assume this equals $N(\Delta\hat{\phi}_{min} \geq 4.0)/N(\Delta\hat{\phi}_{min} < 4.0)$ for QCD events at all E_T^{miss} values, also for samples with b jets such as our signal samples.

To perform this measurement, we divide the data into sideband and signal regions in the $\Delta\hat{\phi}_{min}$-E_T^{miss} plane, as illustrated schematically in Fig. 7. We use the low-E_T^{miss} interval defined by $50 < E_T^{miss} < 100$ GeV and $\Delta\hat{\phi}_{min} >$ 4.0. We call this interval the low sideband (LSB) region. We also define low $\Delta\hat{\phi}_{min}$ (LDP) intervals $\Delta\hat{\phi}_{min} < 4.0$. We do this not only for the $50 < E_T^{miss} < 100$ GeV region, but also for the signal (SIG) regions and for a sideband (SB) region defined by $150 < E_T^{miss} < 250$ GeV. We denote these
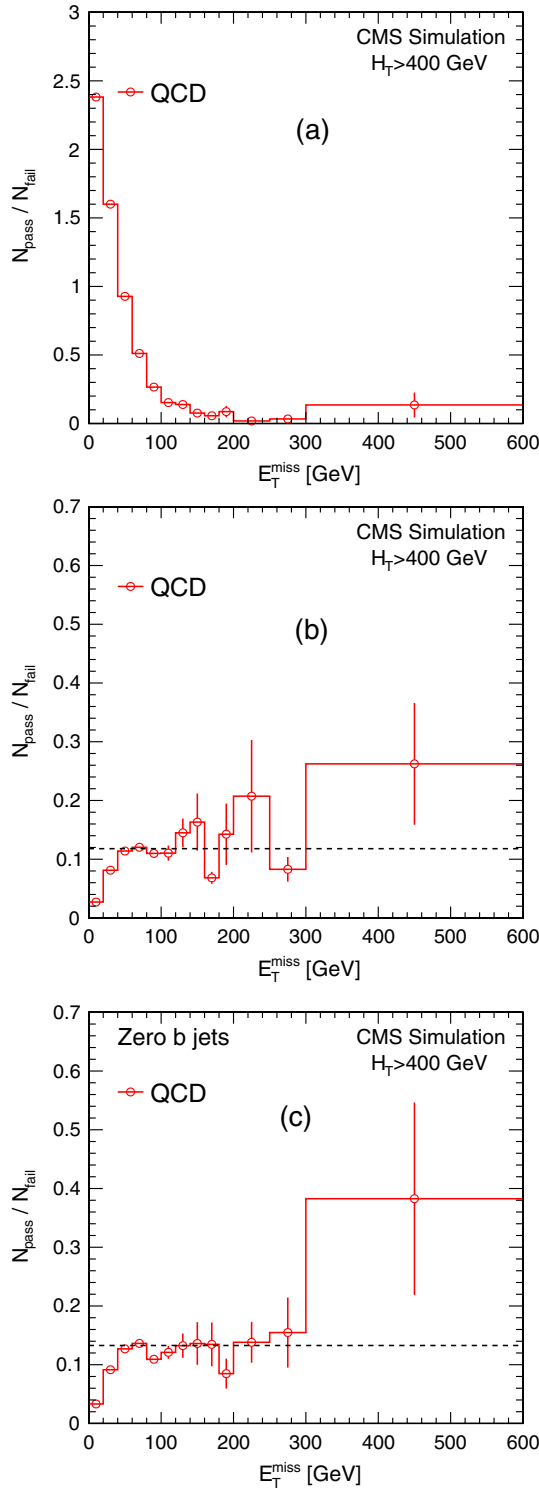
FIG. 5 (color online). QCD-simulation results: (a) The ratio of the number of events that pass the criterion $\Delta\phi_{\min} \geq 0.3$ (N_{pass}) to the number that fail (N_{fail}) as a function of E_T^{miss}, for events selected with the 1BL requirements except for those on $\Delta\hat{\phi}_{\min}$ and E_T^{miss}; (b) The analogous ratio of events with $\Delta\hat{\phi}_{\min} \geq 4.0$ to those with $\Delta\hat{\phi}_{\min} < 4.0$; and (c) the same as (b) for events with zero b jets. The QCD-background estimate is based on the relative flatness of the distributions in (b) and (c) for $E_T^{\text{miss}} \gtrsim 30$ GeV, as illustrated schematically by the horizontal dashed lines.
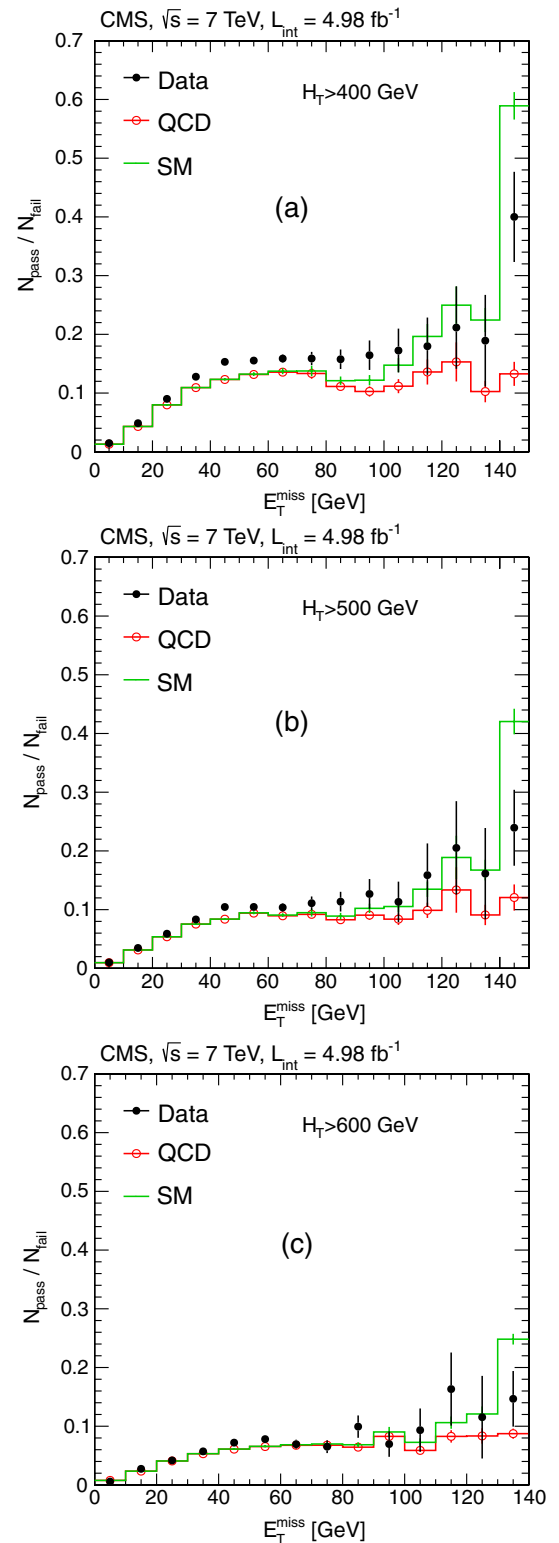
FIG. 6 (color online). The ratio $N(\Delta\hat{\phi}_{\min} \geq 4.0)/N(\Delta\hat{\phi}_{\min} < 4.0)$, denoted $N_{\text{pass}}/N_{\text{fail}}$, as a function of E_T^{miss} for the zero-b-jet sample, for events selected with the basic event-selection criteria of the analysis except for the requirements on E_T^{miss} and the number of b jets. The results are shown for (a) $H_T > 400$ GeV, (b) $H_T > 500$ GeV, and (c) $H_T > 600$ GeV. The histograms show simulated predictions for the QCD and total SM background.

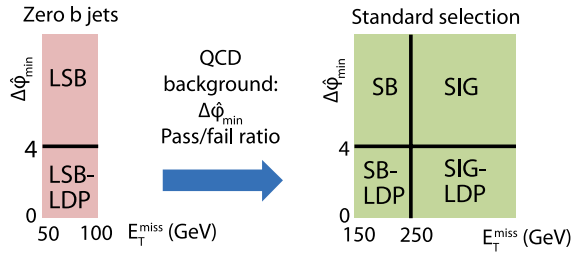FIG. 7 (color online). Schematic diagram illustrating the regions used to evaluate the QCD background. The low sideband (LSB) and low sideband-low $\Delta\hat{\phi}_{\min}$ (LSB-LDP) regions correspond to $50 < E_T^{\mathrm{miss}} < 100$ GeV. The sideband (SB) and sideband-low $\Delta\hat{\phi}_{\min}$(SB-LDP) regions correspond to $150 < E_T^{\mathrm{miss}} < 250$ GeV. The signal (SIG) and signal-low $\Delta\hat{\phi}_{\min}$ (SIG-LDP) regions have E_T^{miss} ranges corresponding to those in Table I. The designation "SIG" generically refers to any of the signal regions in Table I. The SIG and SIG-LDP regions shown in the diagram explicitly depict the loose kinematic signal regions 1BL, 2BL, and 3B, which require $E_T^{\mathrm{miss}} > 250$ GeV, but implicitly include the tight kinematic signal regions 1BT and 2BT, which require $E_T^{\mathrm{miss}} > 500$ GeV and 300 GeV, respectively. For each choice of signal region, the condition on H_T specified in Table I for that region is applied to all six panels of the diagram, while the condition on the number of b jets is applied to the four panels denoted "Standard selection." All regions with the low $\Delta\hat{\phi}_{\min}$ (LDP) designation require $0.0 < \Delta\hat{\phi}_{\min} < 4.0$, while the other regions require $\Delta\hat{\phi}_{\min} > 4.0$.

regions LSB-LDP, SIG-LDP, and SB-LDP, respectively. The LSB-LDP region is dominated by QCD events. Similarly, the SB-LDP and SIG-LDP regions largely consist of QCD events, as illustrated for the 1BL, 2BT, and 3B SIG-LDP regions in Fig. 8. (According to simulation, QCD events comprise between 73% and 85% of the events in the SB-LDP region, depending on the SIG selection; the corresponding results for the SIG-LDP region lie between 50% and 70%.) For higher values of E_T^{miss}, contributions to the SB-LDP and SIG-LDP regions from events with a top quark or a W or Z boson become more important. This contamination is subtracted using simulation.

Applying corrections for the non-QCD components of the SIG-LDP and SB-LDP regions, our estimates of the QCD yields in the SIG and SB regions are therefore

$$N_{\mathrm{SIG}}^{\mathrm{QCD}} = \frac{N_{\mathrm{LSB}}}{N_{\mathrm{LSB\text{-}LDP}}} (N_{\mathrm{SIG\text{-}LDP}} - N_{\mathrm{SIG\text{-}LDP}}^{\mathrm{top,MC}} - N_{\mathrm{SIG\text{-}LDP}}^{\mathrm{W\&Z,MC}}), \quad (1)$$

$$N_{\mathrm{SB}}^{\mathrm{QCD}} = \frac{N_{\mathrm{LSB}}}{N_{\mathrm{LSB\text{-}LDP}}} (N_{\mathrm{SB\text{-}LDP}} - N_{\mathrm{SB\text{-}LDP}}^{\mathrm{top,MC}} - N_{\mathrm{SB\text{-}LDP}}^{\mathrm{W\&Z,MC}}), \quad (2)$$

where the LSB and LSB-LDP results are derived from the zero-b-jet, prescaled H_T trigger sample mentioned in Sec. IV. The result for $N_{\mathrm{SB}}^{\mathrm{QCD}}$ is used in Sec. V C. The ratio $N_{\mathrm{LSB}}/N_{\mathrm{LSB\text{-}LDP}}$ is found to depend on the number of primary vertices (PV) in the event and thus on the LHC instantaneous luminosity. Before evaluating Eqs. (1) and (2), we therefore reweight the events in the prescaled sample to have the same PV distribution as the standard sample.
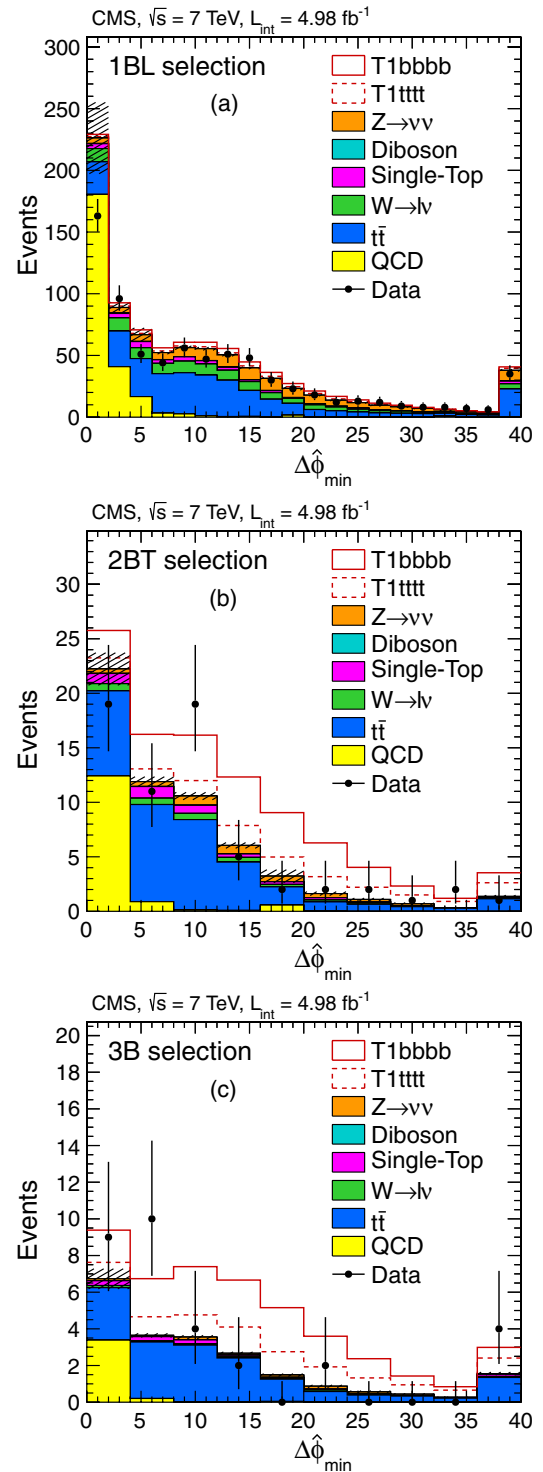
FIG. 8 (color online). The distributions of $\Delta\hat{\phi}_{\min}$ in data and simulation for events selected with the (a) 1BL, (b) 2BT, and (c) 3B requirements, except for the requirement on $\Delta\hat{\phi}_{\min}$. The simulated spectra are normalized as in Fig. 2. The hatched bands show the statistical uncertainty on the total SM prediction from simulation. The open histograms show the expectations for the T1bbbb (solid line) and T1tttt (dashed line) NP models, both with $m_{\tilde{g}} = 925$ GeV, $m_{\mathrm{LSP}} = 100$ GeV, and normalization to NLO + NLL. The SIG-LDP regions correspond to $\Delta\hat{\phi}_{\min} < 4.0$ and the signal (SIG) regions to $\Delta\hat{\phi}_{\min} > 4.0$.

TABLE III. The relative systematic uncertainties (%) for the QCD-background estimate in the signal regions. Because the 1BT QCD-background estimate is zero (Sec. VE), we do not present results for 1BT in this table.

	1BL	2BL	2BT	3B
MC subtraction	23	43	44	24
MC closure	37	41	150	45
LSB reweighting	7.9	7.9	9.8	7.9
Total	44	60	160	52

Systematic uncertainties are summarized in Table III. The systematic uncertainty associated with the subtraction of events with either a top quark or a W or Z boson from the SIG-LDP and SB-LDP regions is determined by varying the subtracted values by their uncertainties, evaluated as described in Sec. VII. The systematic uncertainty associated with the assumption that E_T^{miss} and $\Delta\hat{\phi}_{min}$ are uncorrelated is evaluated with an MC closure test, namely, by determining the ability of the method to predict the correct yield using simulated samples. We compute $(N_{true} - N_{pred})/N_{pred}$, where N_{pred} is the predicted number of QCD events in the signal region, estimated by applying the above procedure to simulated samples treated as data, and N_{true} is the true number. We assign the result, added in quadrature with its statistical uncertainty, as a symmetric systematic uncertainty. This uncertainty is dominated by statistical uncertainties for N_{true}. The closure test is performed both for the standard simulated samples and for simulated samples that are reweighted to account for discrepancies in the jet multiplicity distributions between data and simulation; we take the larger closure discrepancy as the uncertainty. A third systematic uncertainty is evaluated by taking $\pm100\%$ of the shift in the result caused by the PV reweighting of $N_{LSB}/N_{LSB-LDP}$. The systematic uncertainty associated with the trigger efficiency is found to be negligible.

As a cross-check, we vary the definition of the LSB by raising and lowering its lower edge by 10 GeV, which alters the number of events in the LSB by more than a factor of 2 in each case. The observed change in the QCD-background estimate is negligible.

B. Z + jets background

Events with a Z boson and one or more b jets present an irreducible background when the Z decays to two neutrinos. We evaluate this background by reconstructing $Z \rightarrow \ell^+\ell^-$ events ($\ell = e$ or μ) and removing the ℓ^+ and ℓ^-. Fits are performed to determine the $Z \rightarrow \ell^+\ell^-$ yields, which are then corrected for background and efficiency. The efficiency is $\epsilon = \mathcal{A} \cdot \epsilon_{trig} \cdot \epsilon_{\ell reco}^2 \cdot \epsilon_{\ell sel}^2$, where the geometrical acceptance $\mathcal{A}$ is determined from simulation while the trigger ϵ_{trig}, lepton-reconstruction $\epsilon_{\ell reco}$, and lepton-selection $\epsilon_{\ell sel}$ efficiencies are determined from data. The corrected $Z \rightarrow \ell^+\ell^-$ yields are used to estimate the $Z \rightarrow \nu\bar{\nu}$ background through scaling by the ratio of branching fractions, $BR(Z \rightarrow \nu\bar{\nu})/BR(Z \rightarrow \ell^+\ell^-) = 5.95 \pm 0.02$ [32], after accounting for the larger acceptance of $Z \rightarrow \nu\bar{\nu}$ events.

The $Z \rightarrow \ell^+\ell^-$ yields are small or zero in the signal regions. To increase these yields, we select events with the signal-sample requirements except with a significantly looser b-tagging definition. A scale factor derived from a control sample in data is then applied to estimate the number of $Z \rightarrow \ell^+\ell^-$ events in the signal regions. The control sample is defined with the same loosened b-tagging definition, but without requiring the presence of a Z boson, and also by reversing the $\Delta\hat{\phi}_{min}$ requirement, i.e., we require $\Delta\hat{\phi}_{min} < 4.0$, which yields a control sample with a b-jet content similar to that in the $Z \rightarrow \ell^+\ell^-$ and $Z \rightarrow \nu\bar{\nu}$ events. All other selection criteria are the same as for the corresponding signal sample. The scale factors are given by the fraction of events in the control sample that passes the nominal b-tagging requirements. The scale factors have values around 0.30, 0.07, and 0.01 for the samples with ≥ 1, ≥ 2, and ≥ 3 b jets, respectively. We verify that the output of the b-tagging algorithm is independent of the presence of a Z.

We validate our method with a consistency test, applying the above procedure to data samples with loosened restrictions on H_T and E_T^{miss}. We find the number of predicted and observed $Z \rightarrow \ell^+\ell^-$ events to be in close agreement.

Systematic uncertainties are summarized in Table IV. We evaluate a systematic uncertainty on the scale factors by loosening and tightening the b-tagging criterion of the control sample and taking half the difference between

TABLE IV. The relative systematic uncertainties (%) for the $Z \rightarrow \nu\bar{\nu}$ background estimate in the signal regions, determined for $Z \rightarrow e^+e^-$ ($Z \rightarrow \mu^+\mu^-$) events.

	1BL	1BT	2BL	2BT	3B
Scale factors	17 (20)	17 (20)	49 (61)	49 (61)	140 (110)
Nonresonant $\ell^+\ell^-$ background	10 (8)	10 (8)	10 (8)	10 (8)	10 (8)
Acceptance	3 (3)	6 (8)	3 (3)	4 (4)	3 (3)
Lepton-selection efficiency	5 (4)	5 (4)	5 (4)	5 (4)	5 (4)
Trigger efficiency	5 (5)	5 (5)	5 (5)	5 (5)	5 (5)
MC closure	11 (19)	11 (19)	11 (19)	11 (19)	11 (19)
Total	24 (30)	25 (30)	52 (65)	52 (65)	150 (110)

the two results as an uncertainty. The size of the control sample changes by about $\pm 30\%$ in these variations. In addition, we use $\Delta\hat{\phi}_{\min} > 4.0$ rather than $\Delta\hat{\phi}_{\min} < 4.0$ to define the control sample and calculate the difference with respect to the nominal results. Finally, we evaluate the percentage difference between the number of predicted and observed events found with the consistency test described above. The three terms are added in quadrature to define the systematic uncertainty of the scale factors. We evaluate a systematic uncertainty associated with the nonresonant $\ell^+\ell^-$ background to $Z \to \ell^+\ell^-$ events by comparing the fraction of fitted events in the $Z \to \ell^+\ell^-$ peak from the nominal fit with those found using either a loosened H_T or a loosened E_T^{miss} restriction. The rms of the three results is added in quadrature with the statistical uncertainty from the nominal fit to define the systematic uncertainty. The 1BL selection is used to determine this uncertainty for all signal regions. A systematic uncertainty for the acceptance is defined by recalculating the acceptance after varying the p_T and η ranges of the ℓ^+ and ℓ^-. The largest difference with respect to the nominal result is added in quadrature with the statistical uncertainty of the acceptance. A systematic uncertainty is defined for the lepton-selection efficiency, and analogously for the trigger efficiency, by recalculating the respective efficiency after varying the requirements on H_T, $\Delta\hat{\phi}_{\min}$, the number of jets, and the number of b jets. (The number of jets is found using all jets with $p_T > 50$ GeV and $|\eta| < 2.4$.) We also use alternative signal and background shapes in the fits used to extract the $Z \to \ell^+\ell^-$ event yields. The maximum variations from each case are added in quadrature with the statistical uncertainty from the nominal method to define the systematic uncertainties. Finally, we evaluate a systematic uncertainty based on an MC closure test in the manner described in Sec. VA. We use the SB region to determine this uncertainty.

An analogous procedure to that described above is used to evaluate the number of $Z \to \nu\bar{\nu}$ events $N_{\text{SB}}^{Z \to \nu\bar{\nu}}$ in the SB regions ($150 < E_T^{\text{miss}} < 250$ GeV), along with the corresponding uncertainty.

C. Top-quark and W + jets background (nominal)

For most signal regions, $t\bar{t}$ events are expected to be the dominant background (Table II). Backgrounds from single-top-quark and W + jets events are expected to be smaller but to have a similar signature. Almost all top-quark and W + jets background in our analysis arises either because a W boson decays leptonically to an e or a μ, with the e or μ unidentified, not isolated, or outside the acceptance of the analysis, or because a W boson decays to a hadronically decaying τ lepton. We find empirically, through studies with simulation, that the shape of the E_T^{miss} distribution is similar for all top-quark and W + jets background categories that enter the signal (Table I) or sideband ($150 < E_T^{\text{miss}} < 250$ GeV) regions, regardless of whether the W boson

decays to e, μ, or τ, or whether a τ lepton decays hadronically or leptonically: The decay of the W boson in W + jets events generates an E_T^{miss} spectrum (from the neutrino) that is similar to the E_T^{miss} spectrum generated by the W boson produced directly in the decay of a top quark in top-quark events. Additional, softer neutrinos in events with a τ lepton do not much alter this spectrum. We also find that this shape is well-modeled by the E_T^{miss} distribution of a single-lepton (SL) control sample formed by inverting the lepton veto, i.e., by requiring that exactly one e or one μ be present using the lepton-identification criteria of Sec. III, in a sample whose selection is otherwise the same as the corresponding signal sample, except, to reduce the potential contribution of NP to the SL samples, we impose an additional restriction $M_T < 100$ GeV on the SL samples (only), where M_T is the transverse W-boson mass formed from the charged lepton and E_T^{miss} momentum vectors. As an illustration, Fig. 9 shows a comparison based on simulation of the E_T^{miss} distributions in the signal and SL samples, for events selected with the 1BL, 2BT, and 3B criteria.

The E_T^{miss} distributions of events in the SL samples with the 1BL, 2BT, and 3B requirements are shown in Fig. 10. The distributions are seen to be overwhelmingly composed of $t\bar{t}$ events (for example, according to simulation, top and W + jets events comprise over 98% of the events in the SB-SL samples for all SIG selections). The expected contributions of the benchmark T1bbbb NP scenario are found to be negligible, while those of the benchmark T1tttt scenario are seen to be small in Fig. 10 compared to Fig. 3.

Based on these observations, we implement a template method in which the shape of the E_T^{miss} distribution in an SL sample is used to describe the shape of the E_T^{miss} distribution in the corresponding signal sample of Table I, for all top-quark and W + jets categories. An uncertainty for our presumption of the similarity of the E_T^{miss} spectra between different top and W + jet categories is evaluated through the closure test described below. We split each SL sample into a sideband E_T^{miss} region SB-SL defined by $150 < E_T^{\text{miss}} < 250$ GeV, and a signal E_T^{miss} region SIG-SL given by the corresponding E_T^{miss} requirement in Table I. The templates are normalized based on the number of top-quark plus W + jets events observed in the SB regions ($150 < E_T^{\text{miss}} < 250$ GeV) of samples selected with the requirements of Table I except for that on E_T^{miss}. A schematic diagram of the different regions used to evaluate the top and W + jets background with the nominal method is presented in Fig. 11. Contributions to the SB region from QCD and $Z \to \nu\bar{\nu}$ events are taken from the data-based estimates of Secs. VA and VB. Small, residual contributions from other backgrounds such as diboson events are subtracted using simulation.

Our estimate of the top-quark and W + jets background in the SIG region is therefore

$$N_{\text{SIG}}^{\text{top+W}} = \frac{N_{\text{SIG-SL}}}{N_{\text{SB-SL}}}(N_{\text{SB}} - N_{\text{SB}}^{Z \to \nu\bar{\nu}} - N_{\text{SB}}^{\text{QCD}} - N_{\text{SB}}^{\text{other,MC}}). \quad (3)$$
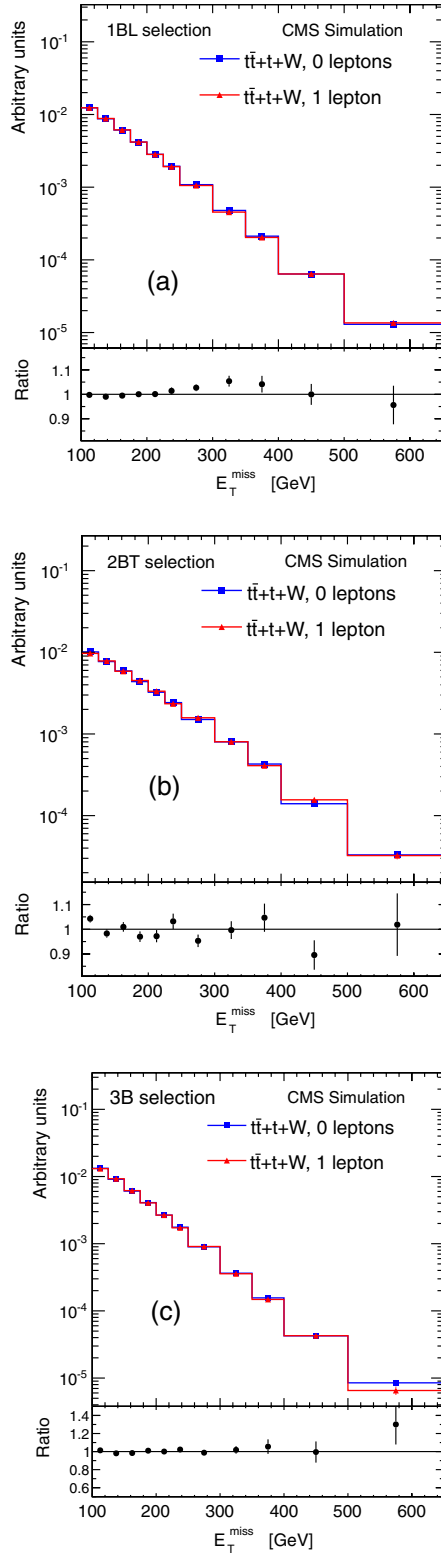
FIG. 9 (color online). The distributions of E_T^{miss} in simulated events selected with the (a) 1BL, (b) 2BT, and (c) 3B requirements, except for the requirement on E_T^{miss}. The square (triangle) symbols show the results for signal (single-lepton SL control) sample events. The small plots below the main figures show the ratio of the signal-to-SL sample curves. The event samples include $t\bar{t}$, W + jet, and single-top-quark events.
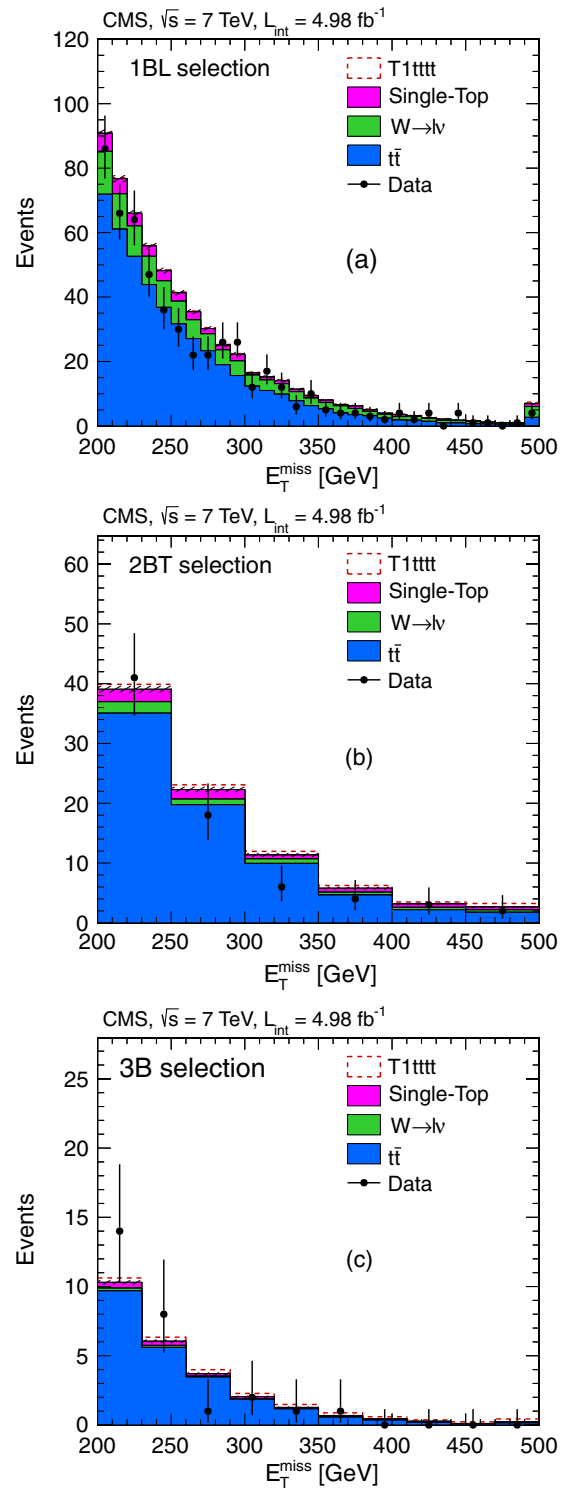
FIG. 10 (color online). The distributions of E_T^{miss} for the SL control sample for events selected with the (a) 1BL, (b) 2BT, and (c) 3B requirements, except for the requirement on E_T^{miss}. The simulated spectra are normalized as in Fig. 2. The hatched bands show the statistical uncertainty on the total SM prediction from simulation. The open dashed histogram shows the expectations for the T1tttt NP model with $m_{\tilde{g}} = 925$ GeV, $m_{LSP} = 100$ GeV, and normalization to NLO + NLL. (The corresponding contributions from the T1bbbb model are negligible and are not shown.)
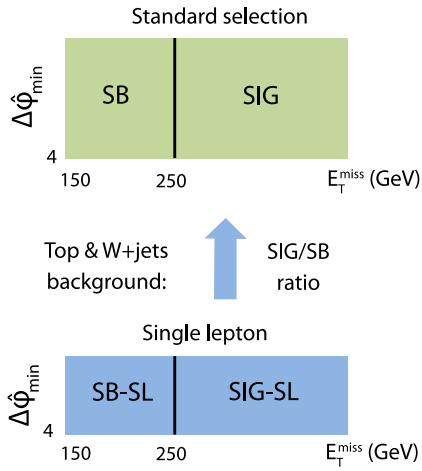
FIG. 11 (color online). Schematic diagram illustrating the regions used to evaluate the top and W + jets background with the nominal method. The sideband (SB) and signal (SIG) regions are as described in the caption to Fig. 7. The sideband-single-lepton (SB-SL) and signal-single-lepton (SIG-SL) regions correspond to the SB and SIG regions, respectively, except an electron or muon is required to be present and a requirement is placed on the transverse W boson mass $M_T < 100$ GeV.

Contamination of the SB region in the benchmark T1bbbb (T1tttt) NP scenario is predicted to be around 1% (1%) for the 1BL, 1BT, and 2BL selections, 4% (3%) for the 2BT selection, and 7% (5%) for the 3B selection. The likelihood procedure described in Sec. VI accounts for NP contributions to all control regions in a coherent manner.

Systematic uncertainties are summarized in Table V. We consider the systematic uncertainty associated with MC closure, evaluated as described in Sec. VA. The closure is evaluated separately for the nominal combined top-quark and W + jets simulated sample, with the W + jets cross section increased by 50% and the single-top-quark cross section by 100%, and with the W + jets cross section decreased by 50% and the single-top-quark cross section by 100%. (These variations account for uncertainties on the relative cross sections; they are based on the uncertainties of the NLO calculations and on comparisons between data and simulation.) We take the largest closure discrepancy as the uncertainty. We also consider the systematic

TABLE V. The relative systematic uncertainties (%) for the nominal top-quark and W + jets background estimate in the signal regions.

	1BL	1BT	2BL	2BT	3B
MC closure	4.6	15	5.4	4.6	2.8
Subtraction of QCD	13	19	8.2	20	8.0
Subtraction of $Z \to \nu\bar{\nu}$	3.4	3.9	5.4	5.9	15
MC subtraction	0.6	0.6	0.2	0.4	0.1
Trigger efficiency	13	14	11	11	10
Total	19	28	15	24	20

uncertainty associated with subtraction of the QCD- and $Z \to \nu\bar{\nu}$-background estimates in the SB region, evaluated by varying these estimates by their uncertainties. The systematic uncertainty associated with other backgrounds is evaluated by varying the MC-based background estimates in the SB region by their uncertainties, which we assume to be $\pm 100\%$ for these small terms. A final systematic uncertainty accounts for the uncertainty on the trigger efficiency.

D. Top-quark and W + jets background (E_T^{miss}-reweighting)

We perform a second, complementary evaluation of the top-quark and W + jets background, which we refer to as the E_T^{miss}-reweighting method. The E_T^{miss} distribution is determined separately for each of the three principal top-quark and W + jets background categories:

(1) top-quark or W + jets events in which exactly one W boson decays into an e or μ, or into a τ that decays into an e or μ, while the other W boson (if any) decays hadronically;

(2) top-quark or W + jets events in which exactly one W boson decays into a hadronically decaying τ, while the other W boson (if any) decays hadronically;

(3) $t\bar{t}$ events in which both W bosons decay into an e, μ, or τ, with the τ decaying either leptonically or hadronically.

For the 1BL selection, these three categories represent, respectively, approximately 44%, 49%, and 7% of the total expected background from top-quark and W + jets events, as determined from simulation.

1. Single e or μ electron or muon events: Category 1

Category 1 top-quark and W + jets background is evaluated with the SL data control sample introduced in Sec. V C. To relate event yields in the SL and SIG samples, we use constraints derived from knowledge of the W-boson polarization. The polarization of the W boson governs the angular distribution of leptons in the W boson rest frame. Because forward-going leptons are boosted to higher momentum and backward-going leptons to lower momentum, the W-boson polarization is directly related to the lepton momentum spectrum in the laboratory frame. W-boson polarization is predicted to high precision in the SM, with calculations carried out to the next-to-next-to-leading order for $t\bar{t}$ events [33] and to NLO for W + jets events [34]. The results of these calculations are consistent with measurements [35–38].

To construct a distribution sensitive to the W-boson polarization in $W \to \ell\bar{\nu}$ ($\ell = e, \mu$) events (we include $W \to \tau\bar{\nu} \to \ell\bar{\nu}\nu\bar{\nu}$ events in this category), we calculate the angle $\Delta\theta_T$ between the direction of the W boson in the laboratory frame and the direction of the e or μ in the W boson rest frame, all defined in the transverse plane.

The p_T of the W boson is given by the vector sum of the E_T^{miss} and charged lepton p_T vectors. When $\Delta\theta_T$ is small, the charged lepton is produced along the p_T direction of the W boson, typically resulting in a high-p_T charged lepton and a low-p_T neutrino (and therefore low E_T^{miss}) in the laboratory frame. Such events usually appear in the SL sample. Conversely, when $\Delta\theta_T$ is large, the charged lepton (neutrino) has lower (higher) p_T, typically leading to larger E_T^{miss}, a charged lepton that fails our e or μ identification criteria, and an event that appears as background in the signal samples.

Figure 12 shows the distribution of $\Delta\theta_T$ in data and simulation for SL events selected with the 1BL, 2BT, and 3B criteria, except a looser E_T^{miss} requirement ($E_T^{miss} >$ 250 GeV) is used for the 2BT region to reduce statistical fluctuations. These results can be compared to those expected in the limit of perfect charged lepton reconstruction, indicated by the dashed histograms in Fig. 12, which show the corresponding simulated predictions, including simulation of the detector, for top-quark and W + jets events with a single $W \to \ell\nu$ decay, where the e or μ needs only to be present at the generator level. The difference between the dashed histogram and the sum of the histograms with exactly one true e or μ found in the event represents $W \to \ell\nu$ events in which the e or μ is either not reconstructed or does not meet the selection criteria of Sec. III.

To estimate the E_T^{miss} distribution of category 1 events, we measure the E_T^{miss} distribution of SL events in bins of $\Delta\theta_T$. The E_T^{miss} distribution for each bin is then multiplied by an MC scale factor, determined as follows. The numerator equals the difference between the total yield from single-lepton processes (the dashed histograms in Fig. 12) and the subset of those events that enter the SL sample, both determined for that bin. The denominator equals the corresponding number of events that appear in the SL sample from all sources. The definition of the denominator therefore corresponds to the SL observable in data. The normalization of the E_T^{miss} distribution in each $\Delta\theta_T$ bin is thus given by the corresponding measured yield, corrected by a scale factor that accounts for the e or μ acceptance and reconstruction efficiency. The corrected E_T^{miss} spectra from the different $\Delta\theta_T$ bins are summed to provide the total E_T^{miss} distribution for category 1 events.

Systematic uncertainties are summarized in Table VI. To evaluate a systematic uncertainty associated with the relative $t\bar{t}$ and W + jets cross sections, we vary the W + jets cross section by $\pm 50\%$. From studies of $Z \to \ell^+\ell^-$ events, the systematic uncertainty associated with the lepton reconstruction efficiency is determined to be 2%. A systematic uncertainty associated with the top-quark p_T spectrum is evaluated by varying the W-boson p_T distribution in the simulated $t\bar{t}$ sample. In these variations, the number of events in the upper 10% of the distribution changes by 2 standard deviations of the corresponding result in data. The systematic uncertainties associated with the jet energy
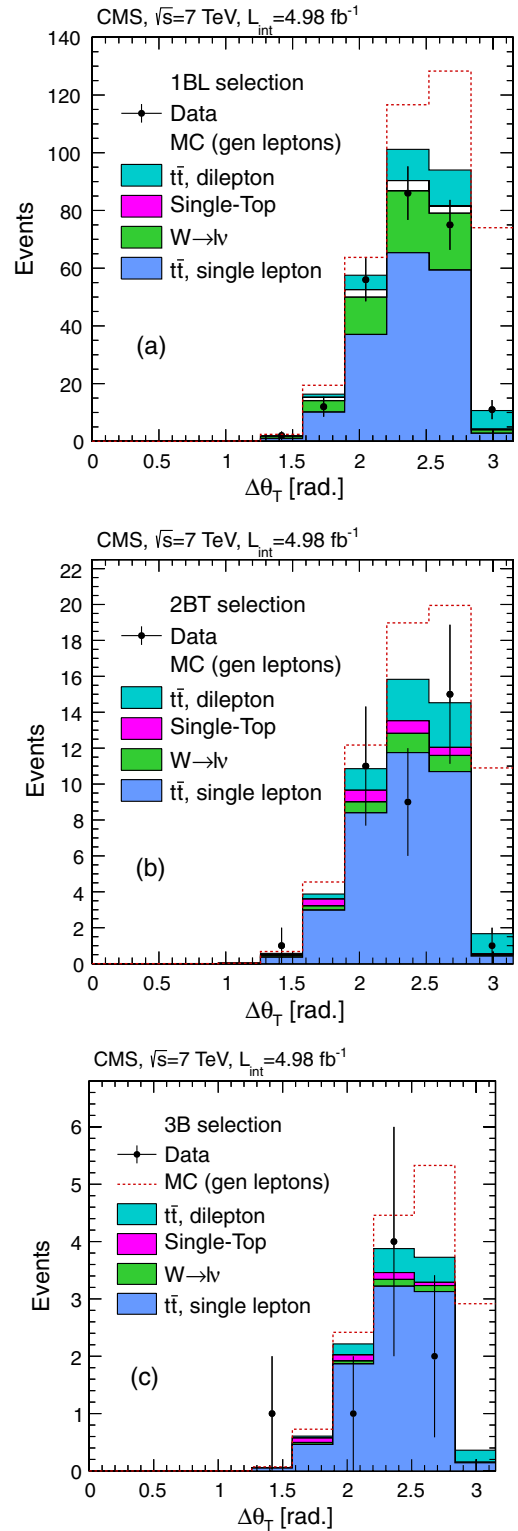

FIG. 12 (color online). The distributions of $\Delta\theta_T$ for events with a single e or μ for the (a) 1BL, (b) 2BT, and (c) 3B selection criteria except with a loosened E_T^{miss} restriction for (b) as described in the text. The stacked, filled histograms show simulated predictions for events in the SL sample. The dashed histogram shows the corresponding simulated prediction in the limit of perfect charged-lepton reconstruction. The simulated results are normalized as in Fig. 2.

TABLE VI.　The relative systematic uncertainties (%) for the $E_{\mathrm{T}}^{\mathrm{miss}}$-reweighting estimate of the top-quark and W + jets background, for category 1 (category 2) events.

	1BL	1BT	2BL	2BT	3B
$\sigma(W \to \ell\nu)/\sigma(t\bar{t})$ ratio	0.1 (0.7)	3.3 (3.9)	0.1 (0.3)	0.2 (0.3)	0.6 (0.3)
Lepton efficiency	2.0 (2.0)	2.0 (2.9)	2.0 (2.0)	2.0 (2.2)	2.0 (2.0)
Top-quark p_{T} spectrum	0.1 (2.2)	6.8 (0.7)	0.6 (3.2)	1.6 (0.7)	1.6 (2.7)
Jet energy scale	1.6 (3.0)	5.0 (5.2)	1.7 (2.1)	1.2 (4.9)	1.1 (4.1)
Jet energy resolution	0.2 (0)	0.4 (1.6)	0.2 (0.2)	0.5 (0.4)	0.3 (0.2)
b-tagging efficiency	0.2 (0.4)	1.0 (2.8)	0.4 (0.6)	0.5 (0.5)	0.3 (0.4)
MC closure	10 (4.7)	55 (29)	12 (5.1)	17 (16)	21 (6.6)
τ visible energy	(1.5)	(3.1)	(1.9)	(2.0)	(2.1)
Total	10 (6.5)	56 (30)	12 (7.0)	17 (17)	21 (8.7)

scale, jet energy resolution, and b-tagging efficiency are evaluated as described in Sec. VII. A systematic uncertainty to account for MC closure is evaluated as described in Sec. V C.

2. $\tau \to$ hadrons: Category 2

Category 2 top-quark and W + jets background is evaluated using a single-muon data control sample. The muon in the event is replaced with a simulated hadronically decaying τ (a τ jet) of the same momentum. To account for the addition of the τ jet, the initial selection criteria are less restrictive than those of the nominal analysis. We require two or more jets, $E_{\mathrm{T}}^{\mathrm{miss}} > 100$ GeV, and do not place restrictions on H_{T} or $\Delta\hat{\phi}_{\mathrm{min}}$. To ensure compatibility with the triggers used to define this single-muon control sample, the minimum muon p_{T} is set to 25 GeV, and the muon isolation requirement is also more stringent than the nominal criterion of Sec. III.

The visible energy fraction of the τ jet, namely, its visible energy divided by its p_{T} value, is determined by sampling p_{T}-dependent MC distributions ("response templates") of the τ visible energy distribution, for a given underlying value of τ lepton p_{T}. The τ jet visible energy is added to the event. The modified event is then subjected to our standard signal region selection criteria. A normalization factor derived from simulation accounts for the relative rates of category 2 and single-muon control sample events.

The same systematic uncertainties are considered as for category 1 events. In addition, we evaluate an uncertainty for the τ-jet visible energy by varying the τ energy scale by $\pm 3\%$ [39]. Systematic uncertainties are summarized in Table VI.

3. $t\bar{t}$ dilepton events: Category 3

The contribution of category 3 top-quark and W + jets background events is determined using dilepton data control samples. When both leptons are electrons or both are muons, or when one is an electron and the other a muon (where the e or μ can be from either a W boson or τ decay), we use simulated predictions to describe the shape of the $E_{\mathrm{T}}^{\mathrm{miss}}$ distribution. The normalization is derived from data, by measuring the number of dilepton events that satisfy loosened selection criteria for each class of events (ee, $\mu\mu$, or $e\mu$) individually. The measured value is multiplied by an MC scale factor, defined by the number of corresponding $t\bar{t}$ dilepton events that satisfy the final selection criteria divided by the number that satisfy the loosened criteria.

When one or both of the leptons is a hadronically decaying τ, we apply a procedure similar to that described for category 2 events. Data control samples of $e\mu$ + jets and $\mu\mu$ + jets events are selected with the loosened criteria of Sec. V D 2. One or both muons is replaced by a τ-jet using MC response templates. The signal-sample selection criteria are applied to the modified events, and the resulting $E_{\mathrm{T}}^{\mathrm{miss}}$ distributions are normalized by scaling the number of events in the respective control samples with factors derived from MC simulation.

The $E_{\mathrm{T}}^{\mathrm{miss}}$ distributions of all six dilepton categories are summed to provide the total category 3 prediction. A systematic uncertainty is evaluated based on MC closure in the manner described in Sec. V A.

E. Summary of the data-based background estimates

A summary of the background estimates is given in Table VII. The results from the three categories of Sec. V D are summed to provide the total $E_{\mathrm{T}}^{\mathrm{miss}}$-reweighting top-quark and W + jets prediction. The estimates from the $E_{\mathrm{T}}^{\mathrm{miss}}$-reweighting method are seen to be consistent with those from the nominal method and to yield smaller uncertainties. Note that there are statistical correlations between the nominal and $E_{\mathrm{T}}^{\mathrm{miss}}$-reweighting methods because they both make use of the SIG-SL region of Fig. 11. However, the nominal method relies on the SB and SB-SL regions of Fig. 11, while the $E_{\mathrm{T}}^{\mathrm{miss}}$-reweighting method does not. The $E_{\mathrm{T}}^{\mathrm{miss}}$-reweighting method makes use of MC scale factors and data selected with lepton-based triggers (for category 2 and 3 events), while the nominal method does not. Furthermore, the systematic uncertainties of the two methods are largely uncorrelated (compare Tables V and VI).

TABLE VII. The SM background estimates from the procedures of Secs. VA, V B, V C, and V D in comparison with the observed number of events in data. The first uncertainties are statistical and the second systematic. For the total SM estimates, we give the results based on both the nominal and the E_T^{miss}-reweighting methods to evaluate the top-quark and $W + $ jets background.

	1BL	1BT	2BL	2BT	3B
QCD	$28 \pm 3 \pm 12$	$0.0 \pm 0.2 \pm 0.3$	$4.7 \pm 1.3 \pm 2.8$	$0.8 \pm 0.4 \pm 1.2$	$1.0 \pm 0.5 \pm 0.5$
$Z \to \nu\bar{\nu}$	$154 \pm 20 \pm 32$	$2.4 \pm 1.9 \pm 0.5$	$32 \pm 5 \pm 20$	$6.2 \pm 2.0 \pm 3.9$	$4.7 \pm 1.3 \pm 6.5$
top-quark and $W + $ jets:					
nominal	$337 \pm 30 \pm 63$	$6.5 \pm 3.3 \pm 1.8$	$123 \pm 17 \pm 19$	$22.8 \pm 6.9 \pm 5.5$	$8.8 \pm 4.0 \pm 1.8$
E_T^{miss}-reweighting	$295 \pm 16 \pm 17$	$4.0 \pm 1.2 \pm 1.5$	$116 \pm 8 \pm 8$	$19.8 \pm 2.5 \pm 2.2$	$13.6 \pm 3.2 \pm 1.2$
Total SM:					
nominal	$519 \pm 36 \pm 72$	$8.9 \pm 3.8 \pm 1.9$	$159 \pm 18 \pm 28$	$29.8 \pm 7.2 \pm 6.8$	$14.4 \pm 4.2 \pm 6.8$
E_T^{miss}-reweighting	$477 \pm 26 \pm 38$	$6.4 \pm 2.3 \pm 1.6$	$153 \pm 10 \pm 22$	$26.8 \pm 3.2 \pm 4.6$	$19.3 \pm 3.5 \pm 6.6$
Data	478	11	146	45	22

The data are generally in good agreement with the SM expectations. However, for 2BT, the data lie 1.1 and 2.2 standard deviations (σ) above the predictions (including systematic uncertainties) for the nominal and E_T^{miss}-reweighting methods, respectively. For 3B, the corresponding deviations are 1.2σ and 0.7σ. Since these deviations are not significant, we do not consider them further.

As an illustration, Fig. 13 presents the background predictions in comparison to data for the 1BL, 2BT, and 3B selections. These results are based on the nominal top-quark and $W + $ jets background estimate.

VI. LIKELIHOOD ANALYSIS

We perform a global likelihood fit that simultaneously determines the SM background and yield of a NP model, using the background estimation techniques of Sec. V. The likelihood analysis allows us to treat the SM backgrounds in a more unified manner than is possible through the collection of individual results in Table VII. Furthermore, it allows us to account for NP contributions to the control regions ("signal contamination"), as well as to the signal region, in a comprehensive and consistent manner.

It is difficult to account for signal contamination using the E_T^{miss}-reweighting method, in contrast to the nominal method. Therefore, signal contamination is evaluated for the nominal method only. Of the two NP scenarios we consider, one of them, the T1tttt model, exhibits non-negligible contamination of the SL samples, while the other, the T1bbbb model, does not. Since the T1bbbb model does not exhibit significant signal contamination, we employ both the nominal- and E_T^{miss}-reweighting-based likelihood fits for this model. For the T1tttt model, we employ only the likelihood fit based on the nominal method.

For the nominal method, the data are divided into 11 mutually exclusive bins, corresponding to the 11 observables listed in Table VIII, where each "observable" corresponds to the number of data events recorded for that bin.

Note that the SB-SL events of Fig. 11 are divided into two components, one for electrons (denoted SB-Se) and the other for muons (denoted SB-Sμ), because their trigger efficiencies and uncertainties differ. Similarly, the reconstruction efficiencies of $Z \to e^+e^-$ and $Z \to \mu^+\mu^-$ events differ, so we divide the $Z \to \ell^+\ell^-$ events of Sec. V B according to the lepton flavor. We further divide the $Z \to \ell^+\ell^-$ events according to whether they appear in the sideband ($150 < E_T^{miss} < 250$ GeV) or signal regions (Table I) of E_T^{miss}. The four $Z \to \ell^+\ell^-$ samples are denoted SIG-ee and SIG-$\mu\mu$ for events in the signal regions, and SB-ee and SB-$\mu\mu$ for events in the sideband region.

The likelihood model provides a prediction for the mean expected value of each observable in terms of the parameters of the signal and background components. The likelihood function is the product of 11 Poisson probability density functions, one for each observable, β distributions [40] that parametrize efficiencies and acceptances, and β' distributions [40] that account for systematic uncertainties and uncertainties on external parameters. (External parameters include such quantities as the acceptance $\mathcal{A}$ and scale factors between the samples with loose and nominal b-tagging requirements discussed in Sec. V B.) The new physics scenarios considered here can contribute significantly to the seven observables listed in the upper portion of Table VIII. In our model, the relative contributions of NP to these seven observables are taken from the NP model under consideration. The NP yield in the SIG bin is a free parameter. The NP contributions to the other six bins thus depend on the NP yield in the SIG bin.

Analogous procedures are used to define the likelihood function for the E_T^{miss}-reweighting method, with simplifications since there is no SB region in this case.

The likelihood function is used to set limits on NP models. Upper limits at 95% confidence level (C.L.) are evaluated taking into account the effects of variation of the external parameters and their correlations. All upper limits are determined using a modified frequentist technique (CL_s) [41,42].
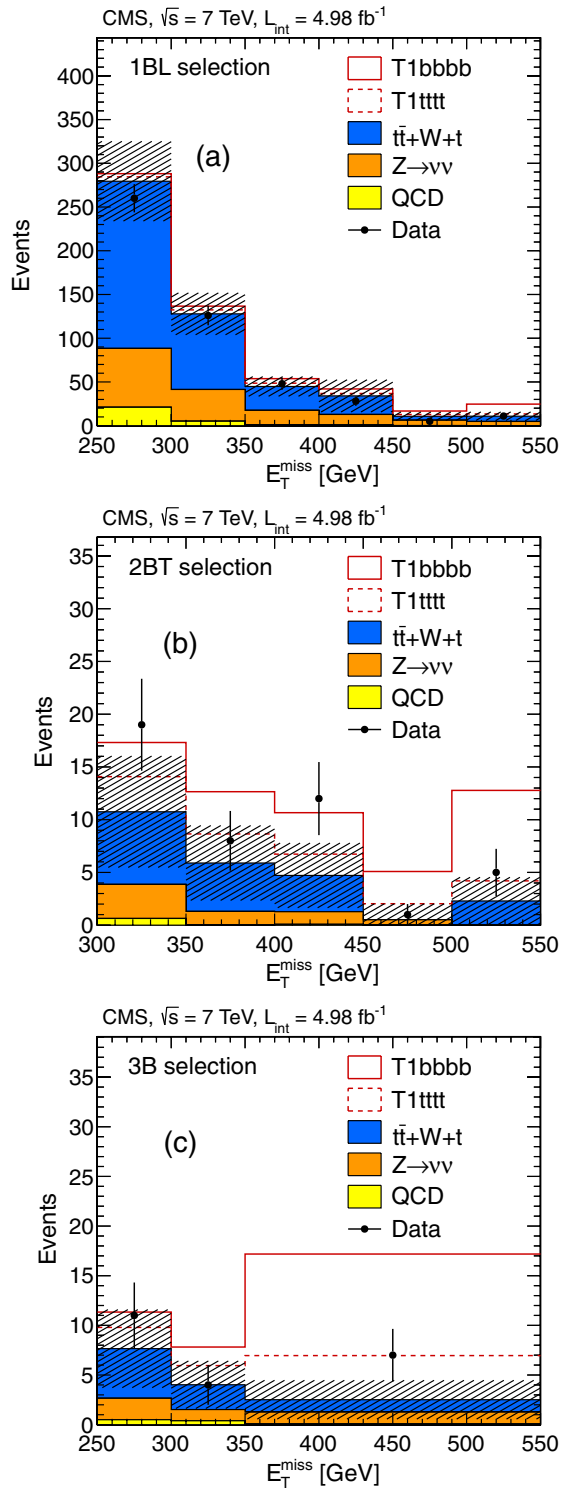
FIG. 13 (color online). The data-based SM background predictions for E_T^{miss} in the (a) 1BL, (b) 2BT, and (c) 3B signal regions in comparison to data. The top-quark and W + jets estimate is based on the nominal method. The hatched bands show the total uncertainty on the prediction, including systematic uncertainties. The uncertainties are correlated between bins. The open histograms show the expectations for the T1bbbb (solid line) and T1tttt (dashed line) NP models, both with $m_{\tilde{g}} = 925$ GeV, $m_{LSP} = 100$ GeV, and normalization to NLO + NLL.

TABLE VIII. The observables (number of data events) of the likelihood analysis for the nominal method, representing the signal region and ten control regions. The seven observables listed in the upper portion of the table are subject to contributions from the signal model in our analysis. The E_T^{miss} SB region corresponds to $150 < E_T^{miss} < 250$ GeV while the SIG regions correspond to the E_T^{miss} regions listed in Table I. The low $\Delta\hat{\phi}_{min}$ region corresponds to $\Delta\hat{\phi}_{min} < 4.0$.

SIG	Standard selection, E_T^{miss} SIG region
SB	Standard selection, E_T^{miss} SB region
SIG-LDP	Standard selection, E_T^{miss} SIG/low $\Delta\hat{\phi}_{min}$ region
SB-LDP	Standard selection, E_T^{miss} SB/low $\Delta\hat{\phi}_{min}$ region
SIG-SL	Single-lepton selection, E_T^{miss} SIG region
SB-S*e*	Single-electron selection, E_T^{miss} SB region
SB-S*μ*	Single-muon selection, E_T^{miss} SB region
SIG-*ee*	$Z \rightarrow e^+e^-$ selection, E_T^{miss} SIG region
SB-*ee*	$Z \rightarrow e^+e^-$ selection, E_T^{miss} SB region
SIG-$\mu\mu$	$Z \rightarrow \mu^+\mu^-$ selection, E_T^{miss} SIG region
SB-$\mu\mu$	$Z \rightarrow \mu^+\mu^-$ selection, E_T^{miss} SB region

VII. LIMITS ON THE T1BBBB AND T1TTTT MODELS

Simulated T1bbbb and T1tttt event samples are generated for a range of gluino and LSP masses using PYTHIA, with $m_{LSP} < m_{\tilde{g}}$. For increased efficiency when performing scans over the SMS parameter space (see below), we base simulation of the CMS detector response on the fast simulation program [43], accounting for modest differences observed with respect to the GEANT4 simulation.

Systematic uncertainties on signal efficiency are summarized in Table IX, using the T1bbbb benchmark model as an example. A systematic uncertainty associated with the jet energy scale is evaluated by varying this scale by its p_T- and η-dependent uncertainties. A systematic uncertainty associated with unclustered energy is evaluated by varying the transverse energy in an event that is not clustered into a

TABLE IX. The relative systematic uncertainties (%) for the signal efficiency of the T1bbbb SMS model with $m_{\tilde{g}} = 925$ GeV and $m_{LSP} = 100$ GeV.

	1BL	1BT	2BL	2BT	3B
Jet energy scale	2.1	11	2.1	3.5	1.9
Unclustered energy	0.2	0.8	0.2	0.2	0.2
Jet energy resolution	1.0	2.0	1.0	1.0	1.0
Pileup	1.0	1.0	1.0	1.0	1.0
b-jet tagging efficiency	0.8	0.9	3.8	3.9	9.0
Trigger efficiency	3.6	3.6	3.6	3.6	3.6
Parton distribution functions	0.4	1.6	0.4	0.7	0.5
Anomalous E_T^{miss}	1.0	1.0	1.0	1.0	1.0
Lepton veto	3.0	3.0	3.0	3.0	3.0
Luminosity	2.2	2.2	2.2	2.2	2.2
Total uncertainty	5.9	12	7.0	7.6	11

physics object by $\pm 10\%$. The systematic uncertainties associated with the correction to the jet energy resolution, the pileup reweighting method mentioned in Sec. III, the b-jet tagging efficiency scale factor, and the trigger efficiency, are evaluated by varying the respective quantities by their uncertainties. The uncertainty for the trigger efficiency includes a 2.5% uncertainty for the plateau efficiency. Systematic uncertainties associated with the parton distribution functions are evaluated following the recommendations of Ref. [44]. The systematic uncertainty associated with anomalous E_T^{miss} values, caused by beam background and reconstruction effects, is 1%. The systematic uncertainty associated with the lepton veto is determined from studies of $Z \to \ell^+\ell^-$ events in data to be 3.0%. The uncertainty in the luminosity determination is 2.2% [45].

We determine 95% C.L. upper limits on the SMS cross sections as a function of the gluino and LSP masses. Using the NLO + NLL cross section as a reference, we also evaluate 95% C.L. exclusion curves. The jet energy scale, unclustered energy, parton distribution function, and b-jet tagging efficiency uncertainties are evaluated for each scan point. Other uncertainties are fixed to the values in Table IX. For each choice of gluino and LSP mass, we use the combination of the top-quark and W + jets background estimation method and the signal selection (Table I) that provides the best expected limit. We do not include results for points near the $m_{\tilde{g}} = m_{\text{LSP}}$ diagonal because of neglected uncertainties from initial-state radiation (ISR), which are large in this region. Specifically, we remove from consideration any point for which the signal efficiency changes by more than 50% when the ISR radiation in PYTHIA is (effectively) turned off.

For the T1bbbb model, the E_T^{miss}-reweighting method is always found to provide the best expected result: We therefore use this method to determine the T1bbbb limits. The E_T^{miss}-reweighting method incorporates an additional constraint compared to the nominal method, namely, the normalization of the SM prediction for the E_T^{miss} distribution from the SIG-SL sample (Fig. 11), and not merely the E_T^{miss} distribution shape. As a consequence, it has greater discrimination power against NP scenarios.

The results for T1bbbb are shown in Fig. 14(a). The 1BT selection is found to provide the best expected result in the bottom right corner of the distribution, corresponding to the region of large gluino-LSP mass splitting. The 2BT selection is best for the swath roughly parallel to the diagonal defined by gluino masses between around 650 and 900 GeV along the bottom edge of the plot. The 3B selection is generally best elsewhere. The solid contour shows the 95% C.L. exclusion curve for the reference cross section. The zigzagging structure around $m_{\tilde{g}} = 900$ GeV, $m_{\text{LSP}} = 450$ GeV is due to the transition from the region where 3B is the best expected selection to that where 2BT is best, in conjunction with the slight excess observed in data for the 2BT selection in comparison with the SM
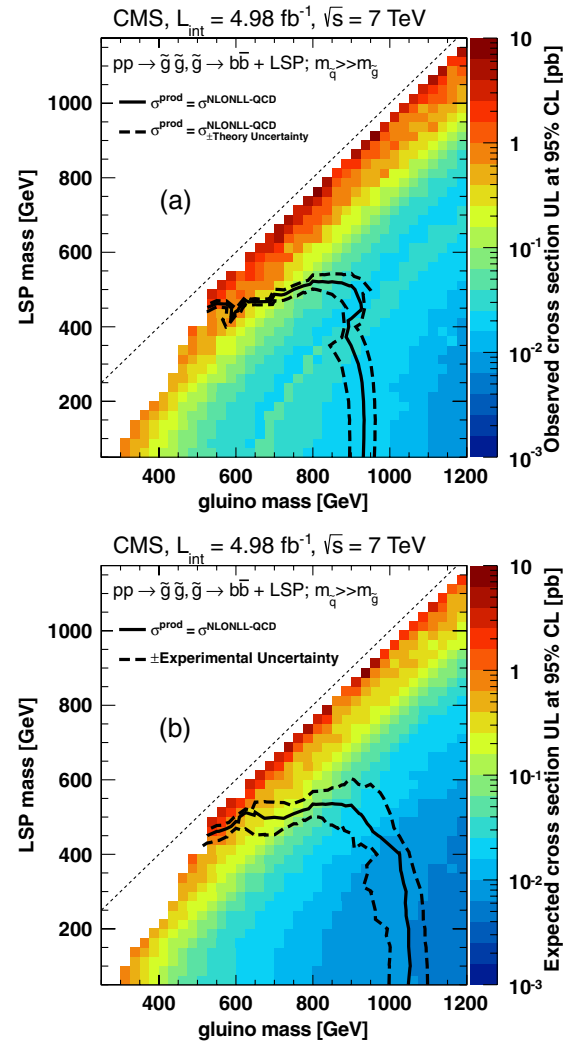

FIG. 14 (color online). (a) The 95% C.L. observed cross-section upper limits (UL) for the T1bbbb SMS model, based on the E_T^{miss}-reweighting method to evaluate the top-quark and W + jets background. For each point, the selection that provides the best expected cross-section limit is used. The solid contour shows the 95% C.L. exclusion limits on the gluino and LSP masses using the NLO + NLL cross section for new physics. The dashed contours represent the theory uncertainties. (b) The corresponding expected limits. The dashed contours represent the uncertainties on the SM background estimates.

prediction for the E_T^{miss}-reweighting method (Sec. V E). The dashed contours represent the results when the reference cross section is varied by the theory uncertainty [46]. Our results improve those of Ref. [7] for large LSP mass values. For example, for gluino masses around 800 GeV, we extend the exclusion of the reference cross section from an LSP mass of about 400 GeV [7] to about 500 GeV, where these numerical values are given by the observed results minus the 1 standard deviation theory uncertainties.

Figure 14(b) shows the best expected results for the T1bbbb model. In this case, the dashed contours represent
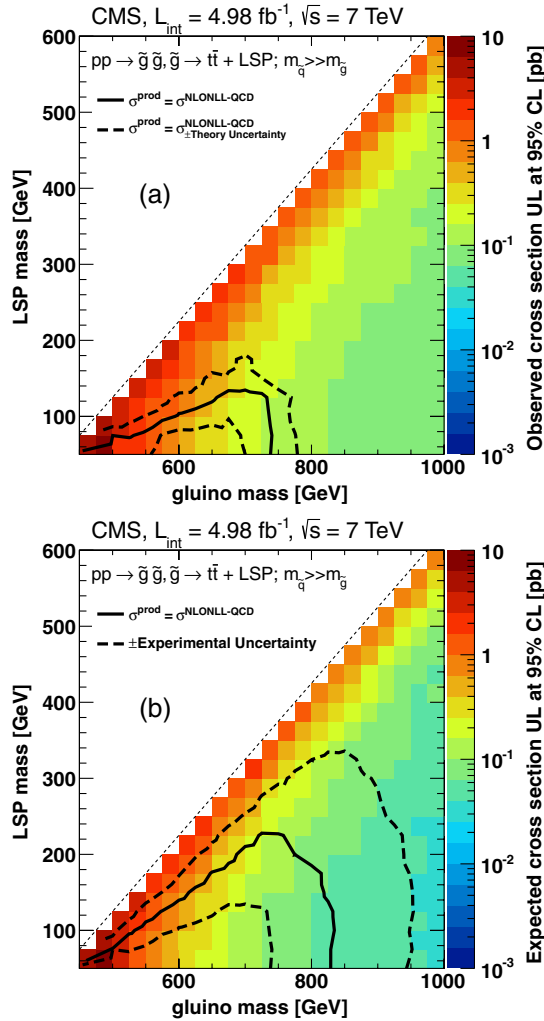
FIG. 15 (color online). (a) The 95% C.L. observed cross-section upper limits (UL) for the T1tttt SMS model, based on the nominal method to evaluate the top-quark and W + jets background. For each point, the selection that provides the best expected cross-section limit is used. (The best selection is virtually always 3B.) The solid contour shows the 95% C.L. exclusion limits on the gluino and LSP masses using the NLO + NLL cross section for new physics. The dashed contours represent the theory uncertainties. (b) The corresponding expected limits. The dashed contours represent the uncertainties on the SM background estimates.

the results when the SM background estimates (Table VII) are varied by their uncertainties.

Even with the selection requirement against ISR events described above, the effect of ISR events can be significant for T1bbbb scenarios that lie within three or four cell widths of the diagonal, where the size of a cell is indicated by the small boxes visible near the diagonal in Fig. 14. We do not account for the effect of ISR for these scenarios. However, for gluino masses less than around 500 GeV, and for points more than three to four cell widths from the diagonal, the effect of ISR is negligible for the points that

are retained. This includes the entire exclusion region for the NLO + NLL reference cross section.

The corresponding results for the T1tttt model are presented in Fig. 15. Our T1tttt results are based on the nominal top-quark and W + jets background estimation method for the reason stated in Sec. VI. In this case, the best expected selection is essentially always 3B. Note that the observed limits for T1tttt, shown in Fig. 15(a), are not as stringent as the expected limits, shown in Fig. 15(b), because of the slight excess of data events in the 3B sample for the nominal method, compared to the SM expectation (Table VII).

VIII. SUMMARY

In this paper, we present a search for an anomalous rate of events with three or more jets, at least one, two, or three tagged bottom-quark jets, no identified, isolated leptons, and large missing transverse energy E_T^{miss}. The study is based on a sample of proton-proton collision data collected at $\sqrt{s} = 7$ TeV with the CMS detector at the LHC during 2011, corresponding to an integrated luminosity of 4.98 fb^{-1}. The principal standard model backgrounds, arising from top-quark, W + jets, Z + jets, and QCD-multijet events, are evaluated from data. We introduce a variable $\Delta\hat{\phi}_{\mathrm{min}}$ that allows us to address the QCD-multijet background with a simple approach. The top-quark and W + jets background is evaluated with two complementary methods, which yield consistent results. In the E_T^{miss}-reweighting method to evaluate the top-quark and W + jets background, we introduce a technique based on the W polarization in $t\bar{t}$ and W + jets events. Our analysis is performed in a likelihood framework in order to account for backgrounds, and for new physics contamination of the control regions, in a unified and consistent manner.

We find no evidence for a significant excess of events beyond the expectations of the standard model and set limits on new physics in the context of the *b*-jet-rich T1bbbb and T1tttt simplified model spectra, in which new strongly interacting particles decay to two *b*-quark jets, or two *t*-quark jets, plus an undetected particle. For the T1bbbb scenario, our results improve on those of Ref. [7] for large LSP masses.

---

[1] G. R. Farrar and P. Fayet, Phys. Lett. B **76**, 575 (1978).

[2] J. Wess and B. Zumino, Nucl. Phys. **B70**, 39 (1974).

[3] S. P. Martin, arXiv:hep-ph/9709356.

[4] S. Chatrchyan *et al.* (CMS Collaboration), J. High Energy Phys. 07 (2011) 113.

[5] G. Aad *et al.* (ATLAS Collaboration), Phys. Lett. B **701**, 398 (2011).

[6] G. Aad *et al.* (ATLAS Collaboration), Phys. Rev. D **85**, 112006 (2012).

[7] S. Chatrchyan *et al.* (CMS Collaboration), J. High Energy Phys. 10 (2012) 18.

[8] G. Aad *et al.* (ATLAS Collaboration), arXiv:1207.4686.

[9] N. Arkani-Hamed, P. Schuster, N. Toro, J. Thaler, L.-T. Wang, B. Knuteson, and S. Mrenna, arXiv:hep-ph/0703088.

[10] J. Alwall, P. C. Schuster, and N. Toro, Phys. Rev. D **79**, 075020 (2009).

[11] J. Alwall, M.-P. Le, M. Lisanti, and J. G. Wacker, Phys. Rev. D **79**, 015005 (2009).

[12] D. Alves, Daniele Alves, Nima Arkani-Hamed, Sanjay Arora, Yang Bai, Matthew Baumgart, Joshua Berger, Matthew Buckley, Bart Butler, Spencer Chang, Hsin-Chia Cheng *et al.*, J. Phys. G **39**, 105005 (2012).

[13] W. Beenakker, R. Höpker, M. Spira, and P. M. Zerwas, Nucl. Phys. **B492**, 51 (1997).

[14] A. Kulesza and L. Motyka, Phys. Rev. Lett. **102**, 111802 (2009).

[15] A. Kulesza and L. Motyka, Phys. Rev. D **80**, 095004 (2009).

[16] W. Beenakker, S. Brensing, M. Krämer, A. Kulesza, E. Laenen, and I. Niessen, J. High Energy Phys. 12 (2009) 041.

[17] W. Beenakker, S. Brensing, M. Krämer, A. Kulesza, E. Laenen, L. Motyka, and I. Niessen, Int. J. Mod. Phys. A **26**, 2637 (2011).

[18] S. Chatrchyan *et al.* (CMS Collaboration), J. Instrum. **3**, S08004 (2008).

[19] CMS Collaboration, CMS Physics Analysis Summary Report No. CMS-PAS-PFT-09-001, 2009.

[20] M. Cacciari, G. P. Salam, and G. Soyez, J. High Energy Phys. 04 (2008) 063.

[21] S. Chatrchyan *et al.* (CMS Collaboration), J. Instrum. **6**, P11002 (2011).

[22] CMS Collaboration, CMS Physics Analysis Summary Report No. CMS-PAS-TRK-10-005, 2010.

[23] CMS Collaboration, CMS Physics Analysis Summary Report No. CMS-PAS-EGM-10-004, 2010.

[24] S. Chatrchyan *et al.* (CMS Collaboration), JINST **7,** P10002 (2012).

[25] CMS Collaboration, CMS Physics Analysis Summary Report No. CMS-PAS-BTV-11-004, 2012.

[26] J. Alwall, M. Herquet, F. Maltoni, O. Mattelaer, and T. Stelzer, J. High Energy Phys. 06 (2011) 128.

[27] S. Frixione, P. Nason, and C. Oleari, J. High Energy Phys. 11 (2007) 070.

[28] T. Sjöstrand, S. Mrenna, and P. Skands, J. High Energy Phys. 05 (2006) 026.

[29] J. Pumplin, D. R. Stump, J. Huston, H.-L. Lai, P. Nadolsky, and W.-K. Tung, J. High Energy Phys. 07 (2002) 012.

[30] S. Agostinelli, J. Allison, K. Amako, J. Apostolakis, H. Araujo, P. Arce, M. Asai, D. Axen, S. Banerjee, G. Barrand *et al.*, Nucl. Instrum. Methods Phys. Res., Sect. A **506,** 250 (2003).

[31] S. Chatrchyan *et al.* (CMS Collaboration), Phys. Rev. D **84,** 092004 (2011).

[32] K. Nakamura *et al.* (Particle Data Group), J. Phys. G **37,** 075021 (2010).

[33] A. Czarnecki, J. G. Körner, and J. H. Piclum, Phys. Rev. D **81,** 111503 (2010).

[34] Z. Bern, G. Diana, L. J. Dixon, F. Febres Cordero, D. Forde, T. Gleisberg, S. Hoeche, H. Ita, D. A. Kosower, D. Maître, and K. Ozeren, Phys. Rev. D **84,** 034008 (2011).

[35] T. Aaltonen *et al.* (CDF Collaboration), Phys. Rev. Lett. **105,** 042002 (2010).

[36] V. M. Abazov *et al.* (D0 Collaboration), Phys. Rev. D **83,** 032009 (2011).

[37] S. Chatrchyan *et al.* (CMS Collaboration), Phys. Rev. Lett. **107,** 021802 (2011).

[38] G. Aad *et al.* (ATLAS Collaboration), J. High Energy Phys. 06 (2012) 088.

[39] S. Chatrchyan *et al.* (CMS Collaboration), J. Instrum. **7,** P01001 (2012).

[40] N. L. Johnson, S. Kotz, and N. N. Balakrishnan, *Continuous Univariate Distributions* (Wiley Interscience, New York, 1995), Vol. 2.

[41] T. Junk, Nucl. Instrum. Methods Phys. Res., Sect. A **434,** 435 (1999).

[42] A. L. Read, J. Phys. G **28,** 2693 (2002).

[43] CMS Collaboration, CMS Detector Performance Summary Report No. CMS-DP-2010-039 (2010).

[44] M. Botje, J. Butterworth, A. Cooper-Sarkar, A. de Roeck, J. Feltesse, S. Forte, A. Glazov, J. Huston, R. McNulty, and T. Sjöstrand, arXiv:1101.0538.

[45] CMS Collaboration, CMS Physics Analysis Summary Report No. CMS-PAS-SMP-12-008, 2012.

[46] M. Krämer, A. Kulesza, R. van der Leeuw, M. Mangano, S. Padhi, T. Plehn, and X. Portell, arXiv:1206.2892.

S. Chatrchyan,[1] V. Khachatryan,[1] A. M. Sirunyan,[1] A. Tumasyan,[1] W. Adam,[2] E. Aguilo,[2] T. Bergauer,[2]
M. Dragicevic,[2] J. Erö,[2] C. Fabjan,[2,b] M. Friedl,[2] R. Frühwirth,[2,b] V. M. Ghete,[2] J. Hammer,[2] N. Hörmann,[2]
J. Hrubec,[2] M. Jeitler,[2,b] W. Kiesenhofer,[2] V. Knünz,[2] M. Krammer,[2,b] I. Krätschmer,[2] D. Liko,[2] I. Mikulec,[2]
M. Pernicka,[2,a] B. Rahbaran,[2] C. Rohringer,[2] H. Rohringer,[2] R. Schöfbeck,[2] J. Strauss,[2] A. Taurok,[2]
W. Waltenberger,[2] G. Walzel,[2] E. Widl,[2] C.-E. Wulz,[2,b] V. Mossolov,[3] N. Shumeiko,[3] J. Suarez Gonzalez,[3]
M. Bansal,[4] S. Bansal,[4] T. Cornelis,[4] E. A. De Wolf,[4] X. Janssen,[4] S. Luyckx,[4] L. Mucibello,[4] S. Ochesanu,[4]
B. Roland,[4] R. Rougny,[4] M. Selvaggi,[4] Z. Staykova,[4] H. Van Haevermaet,[4] P. Van Mechelen,[4] N. Van Remortel,[4]
A. Van Spilbeeck,[4] F. Blekman,[5] S. Blyweert,[5] J. D'Hondt,[5] R. Gonzalez Suarez,[5] A. Kalogeropoulos,[5] M. Maes,[5]
A. Olbrechts,[5] W. Van Doninck,[5] P. Van Mulders,[5] G. P. Van Onsem,[5] I. Villella,[5] B. Clerbaux,[6] G. De Lentdecker,[6]
V. Dero,[6] A. P. R. Gay,[6] T. Hreus,[6] A. Léonard,[6] P. E. Marage,[6] T. Reis,[6] L. Thomas,[6] G. Vander Marcken,[6]
C. Vander Velde,[6] P. Vanlaer,[6] J. Wang,[6] V. Adler,[7] K. Beernaert,[7] A. Cimmino,[7] S. Costantini,[7] G. Garcia,[7]
M. Grunewald,[7] B. Klein,[7] J. Lellouch,[7] A. Marinov,[7] J. Mccartin,[7] A. A. Ocampo Rios,[7] D. Ryckbosch,[7]
N. Strobbe,[7] F. Thyssen,[7] M. Tytgat,[7] P. Verwilligen,[7] S. Walsh,[7] E. Yazgan,[7] N. Zaganidis,[7] S. Basegmez,[8]
G. Bruno,[8] R. Castello,[8] L. Ceard,[8] C. Delaere,[8] T. du Pree,[8] D. Favart,[8] L. Forthomme,[8] A. Giammanco,[8,c] J. Hollar,[8]
V. Lemaitre,[8] J. Liao,[8] O. Militaru,[8] C. Nuttens,[8] D. Pagano,[8] A. Pin,[8] K. Piotrzkowski,[8] N. Schul,[8]
J. M. Vizan Garcia,[8] N. Beliy,[9] T. Caebergs,[9] E. Daubie,[9] G. H. Hammad,[9] G. A. Alves,[10] M. Correa Martins Junior,[10]
D. De Jesus Damiao,[10] T. Martins,[10] M. E. Pol,[10] M. H. G. Souza,[10] W. L. Aldá Júnior,[11] W. Carvalho,[11]
A. Custódio,[11] E. M. Da Costa,[11] C. De Oliveira Martins,[11] S. Fonseca De Souza,[11] D. Matos Figueiredo,[11]
L. Mundim,[11] H. Nogima,[11] V. Oguri,[11] W. L. Prado Da Silva,[11] A. Santoro,[11] L. Soares Jorge,[11] A. Sznajder,[11]
T. S. Anjos,[12,d] C. A. Bernardes,[12,d] F. A. Dias,[12,e] T. R. Fernandez Perez Tomei,[12] E. M. Gregores,[12,d] C. Lagana,[12]
F. Marinho,[12] P. G. Mercadante,[12,d] S. F. Novaes,[12] Sandra S. Padula,[12] V. Genchev,[13,f] P. Iaydjiev,[13,f] S. Piperov,[13]
M. Rodozov,[13] S. Stoykova,[13] G. Sultanov,[13] V. Tcholakov,[13] R. Trayanov,[13] M. Vutova,[13] A. Dimitrov,[14]
R. Hadjiiska,[14] V. Kozhuharov,[14] L. Litov,[14] B. Pavlov,[14] P. Petkov,[14] J. G. Bian,[15] G. M. Chen,[15] H. S. Chen,[15]
C. H. Jiang,[15] D. Liang,[15] S. Liang,[15] X. Meng,[15] J. Tao,[15] J. Wang,[15] X. Wang,[15] Z. Wang,[15] H. Xiao,[15] M. Xu,[15]
J. Zang,[15] Z. Zhang,[15] C. Asawatangtrakuldee,[16] Y. Ban,[16] Y. Guo,[16] W. Li,[16] S. Liu,[16] Y. Mao,[16] S. J. Qian,[16]
H. Teng,[16] D. Wang,[16] L. Zhang,[16] W. Zou,[16] C. Avila,[17] J. P. Gomez,[17] B. Gomez Moreno,[17] A. F. Osorio Oliveros,[17]
J. C. Sanabria,[17] N. Godinovic,[18] D. Lelas,[18] R. Plestina,[18,g] D. Polic,[18] I. Puljak,[18,f] Z. Antunovic,[19] M. Kovac,[19]
V. Brigljevic,[20] S. Duric,[20] K. Kadija,[20] J. Luetic,[20] S. Morovic,[20] A. Attikis,[21] M. Galanti,[21] G. Mavromanolakis,[21]

J. Mousa,[21] C. Nicolaou,[21] F. Ptochos,[21] P. A. Razis,[21] M. Finger,[22] M. Finger, Jr.,[22] Y. Assran,[23,h] S. Elgammal,[23,i]
A. Ellithi Kamel,[23,j] S. Khalil,[23,i] M. A. Mahmoud,[23,k] A. Radi,[23,l,m] M. Kadastik,[24] M. Müntel,[24] M. Raidal,[24]
L. Rebane,[24] A. Tiko,[24] P. Eerola,[25] G. Fedi,[25] M. Voutilainen,[25] J. Härkönen,[26] A. Heikkinen,[26] V. Karimäki,[26]
R. Kinnunen,[26] M. J. Kortelainen,[26] T. Lampén,[26] K. Lassila-Perini,[26] S. Lehti,[26] T. Lindén,[26] P. Luukka,[26]
T. Mäenpää,[26] T. Peltola,[26] E. Tuominen,[26] J. Tuominiemi,[26] E. Tuovinen,[26] D. Ungaro,[26] L. Wendland,[26]
K. Banzuzi,[27] A. Karjalainen,[27] A. Korpela,[27] T. Tuuva,[27] M. Besancon,[28] S. Choudhury,[28] M. Dejardin,[28]
D. Denegri,[28] B. Fabbro,[28] J. L. Faure,[28] F. Ferri,[28] S. Ganjour,[28] A. Givernaud,[28] P. Gras,[28]
G. Hamel de Monchenault,[28] P. Jarry,[28] E. Locci,[28] J. Malcles,[28] L. Millischer,[28] A. Nayak,[28] J. Rander,[28]
A. Rosowsky,[28] I. Shreyber,[28] M. Titov,[28] S. Baffioni,[29] F. Beaudette,[29] L. Benhabib,[29] L. Bianchini,[29] M. Bluj,[29,n]
C. Broutin,[29] P. Busson,[29] C. Charlot,[29] N. Daci,[29] T. Dahms,[29] L. Dobrzynski,[29] R. Granier de Cassagnac,[29]
M. Haguenauer,[29] P. Miné,[29] C. Mironov,[29] I. N. Naranjo,[29] M. Nguyen,[29] C. Ochando,[29] P. Paganini,[29] D. Sabes,[29]
R. Salerno,[29] Y. Sirois,[29] C. Veelken,[29] A. Zabi,[29] J.-L. Agram,[30,o] J. Andrea,[30] D. Bloch,[30] D. Bodin,[30]
J.-M. Brom,[30] M. Cardaci,[30] E. C. Chabert,[30] C. Collard,[30] E. Conte,[30,o] F. Drouhin,[30,o] C. Ferro,[30] J.-C. Fontaine,[30,o]
D. Gelé,[30] U. Goerlach,[30] P. Juillot,[30] A.-C. Le Bihan,[30] P. Van Hove,[30] F. Fassi,[31] D. Mercier,[31] S. Beauceron,[32]
N. Beaupere,[32] O. Bondu,[32] G. Boudoul,[32] J. Chasserat,[32] R. Chierici,[32,f] D. Contardo,[32] P. Depasse,[32]
H. El Mamouni,[32] J. Fay,[32] S. Gascon,[32] M. Gouzevitch,[32] B. Ille,[32] T. Kurca,[32] M. Lethuillier,[32] L. Mirabito,[32]
S. Perries,[32] V. Sordini,[32] Y. Tschudi,[32] P. Verdier,[32] S. Viret,[32] Z. Tsamalaidze,[33,p] G. Anagnostou,[34]
C. Autermann,[34] S. Beranek,[34] M. Edelhoff,[34] L. Feld,[34] N. Heracleous,[34] O. Hindrichs,[34] R. Jussen,[34] K. Klein,[34]
J. Merz,[34] A. Ostapchuk,[34] A. Perieanu,[34] F. Raupach,[34] J. Sammet,[34] S. Schael,[34] D. Sprenger,[34] H. Weber,[34]
B. Wittmer,[34] V. Zhukov,[34,q] M. Ata,[35] J. Caudron,[35] E. Dietz-Laursonn,[35] D. Duchardt,[35] M. Erdmann,[35]
R. Fischer,[35] A. Güth,[35] T. Hebbeker,[35] C. Heidemann,[35] K. Hoepfner,[35] D. Klingebiel,[35] P. Kreuzer,[35]
M. Merschmeyer,[35] A. Meyer,[35] M. Olschewski,[35] P. Papacz,[35] H. Pieta,[35] H. Reithler,[35] S. A. Schmitz,[35]
L. Sonnenschein,[35] J. Steggemann,[35] D. Teyssier,[35] M. Weber,[35] M. Bontenackels,[36] V. Cherepanov,[36] Y. Erdogan,[36]
G. Flügge,[36] H. Geenen,[36] M. Geisler,[36] W. Haj Ahmad,[36] F. Hoehle,[36] B. Kargoll,[36] T. Kress,[36] Y. Kuessel,[36]
A. Nowack,[36] L. Perchalla,[36] O. Pooth,[36] P. Sauerland,[36] A. Stahl,[36] M. Aldaya Martin,[37] J. Behr,[37] W. Behrenhoff,[37]
U. Behrens,[37] M. Bergholz,[37,r] A. Bethani,[37] K. Borras,[37] A. Burgmeier,[37] A. Cakir,[37] L. Calligaris,[37] A. Campbell,[37]
E. Castro,[37] F. Costanza,[37] D. Dammann,[37] C. Diez Pardos,[37] G. Eckerlin,[37] D. Eckstein,[37] G. Flucke,[37] A. Geiser,[37]
I. Glushkov,[37] P. Gunnellini,[37] S. Habib,[37] J. Hauk,[37] G. Hellwig,[37] H. Jung,[37] M. Kasemann,[37] P. Katsas,[37]
C. Kleinwort,[37] H. Kluge,[37] A. Knutsson,[37] M. Krämer,[37] D. Krücker,[37] E. Kuznetsova,[37] W. Lange,[37]
W. Lohmann,[37,r] B. Lutz,[37] R. Mankel,[37] I. Marfin,[37] M. Marienfeld,[37] I.-A. Melzer-Pellmann,[37] A. B. Meyer,[37]
J. Mnich,[37] A. Mussgiller,[37] S. Naumann-Emme,[37] O. Novgorodova,[37] J. Olzem,[37] H. Perrey,[37] A. Petrukhin,[37]
D. Pitzl,[37] A. Raspereza,[37] P. M. Ribeiro Cipriano,[37] C. Riedl,[37] E. Ron,[37] M. Rosin,[37] J. Salfeld-Nebgen,[37]
R. Schmidt,[37,r] T. Schoerner-Sadenius,[37] N. Sen,[37] A. Spiridonov,[37] M. Stein,[37] R. Walsh,[37] C. Wissing,[37]
V. Blobel,[38] J. Draeger,[38] H. Enderle,[38] J. Erfle,[38] U. Gebbert,[38] M. Görner,[38] T. Hermanns,[38] R. S. Höing,[38]
K. Kaschube,[38] G. Kaussen,[38] H. Kirschenmann,[38] R. Klanner,[38] J. Lange,[38] B. Mura,[38] F. Nowak,[38] T. Peiffer,[38]
N. Pietsch,[38] D. Rathjens,[38] C. Sander,[38] H. Schettler,[38] P. Schleper,[38] E. Schlieckau,[38] A. Schmidt,[38] M. Schröder,[38]
T. Schum,[38] M. Seidel,[38] V. Sola,[38] H. Stadie,[38] G. Steinbrück,[38] J. Thomsen,[38] L. Vanelderen,[38] C. Barth,[39]
J. Berger,[39] C. Böser,[39] T. Chwalek,[39] W. De Boer,[39] A. Descroix,[39] A. Dierlamm,[39] M. Feindt,[39] M. Guthoff,[39,f]
C. Hackstein,[39] F. Hartmann,[39] T. Hauth,[39,f] M. Heinrich,[39] H. Held,[39] K. H. Hoffmann,[39] S. Honc,[39] I. Katkov,[39,q]
J. R. Komaragiri,[39] P. Lobelle Pardo,[39] D. Martschei,[39] S. Mueller,[39] Th. Müller,[39] M. Niegel,[39] A. Nürnberg,[39]
O. Oberst,[39] A. Oehler,[39] J. Ott,[39] G. Quast,[39] K. Rabbertz,[39] F. Ratnikov,[39] N. Ratnikova,[39] S. Röcker,[39]
A. Scheurer,[39] F.-P. Schilling,[39] G. Schott,[39] H. J. Simonis,[39] F. M. Stober,[39] D. Troendle,[39] R. Ulrich,[39]
J. Wagner-Kuhr,[39] S. Wayand,[39] T. Weiler,[39] M. Zeise,[39] G. Daskalakis,[40] T. Geralis,[40] S. Kesisoglou,[40]
A. Kyriakis,[40] D. Loukas,[40] I. Manolakos,[40] A. Markou,[40] C. Markou,[40] C. Mavrommatis,[40] E. Ntomari,[40]
L. Gouskos,[41] T. J. Mertzimekis,[41] A. Panagiotou,[41] N. Saoulidou,[41] I. Evangelou,[42] C. Foudas,[42] P. Kokkas,[42]
N. Manthos,[42] I. Papadopoulos,[42] V. Patras,[42] G. Bencze,[43] C. Hajdu,[43] P. Hidas,[43] D. Horvath,[43,s] F. Sikler,[43]
V. Veszpremi,[43] G. Vesztergombi,[43,t] N. Beni,[44] S. Czellar,[44] J. Molnar,[44] J. Palinkas,[44] Z. Szillasi,[44] J. Karancsi,[45]
P. Raics,[45] Z. L. Trocsanyi,[45] B. Ujvari,[45] S. B. Beri,[46] V. Bhatnagar,[46] N. Dhingra,[46] R. Gupta,[46] M. Kaur,[46]
M. Z. Mehta,[46] N. Nishu,[46] L. K. Saini,[46] A. Sharma,[46] J. Singh,[46] Ashok Kumar,[47] Arun Kumar,[47] S. Ahuja,[47]
A. Bhardwaj,[47] B. C. Choudhary,[47] S. Malhotra,[47] M. Naimuddin,[47] K. Ranjan,[47] V. Sharma,[47] R. K. Shivpuri,[47]
S. Banerjee,[48] S. Bhattacharya,[48] S. Dutta,[48] B. Gomber,[48] Sa. Jain,[48] Sh. Jain,[48] R. Khurana,[48] S. Sarkar,[48]

M. Sharan,[48] A. Abdulsalam,[49] R. K. Choudhury,[49] D. Dutta,[49] S. Kailas,[49] V. Kumar,[49] P. Mehta,[49]
A. K. Mohanty,[49,f] L. M. Pant,[49] P. Shukla,[49] T. Aziz,[50] S. Ganguly,[50] M. Guchait,[50,u] M. Maity,[50,v] G. Majumder,[50]
K. Mazumdar,[50] G. B. Mohanty,[50] B. Parida,[50] K. Sudhakar,[50] N. Wickramage,[50] S. Banerjee,[51] S. Dugad,[51]
H. Arfaei,[52] H. Bakhshiansohi,[52,w] S. M. Etesami,[52,x] A. Fahim,[52,w] M. Hashemi,[52] H. Hesari,[52] A. Jafari,[52,w]
M. Khakzad,[52] M. Mohammadi Najafabadi,[52] S. Paktinat Mehdiabadi,[52] B. Safarzadeh,[52,y] M. Zeinali,[52,x]
M. Abbrescia,[53a,53b] L. Barbone,[53a,53b] C. Calabria,[53a,53b,f] S. S. Chhibra,[53a,53b] A. Colaleo,[53a] D. Creanza,[53a,53c]
N. De Filippis,[53a,53c,f] M. De Palma,[53a,53b] L. Fiore,[53a] G. Iaselli,[53a,53c] L. Lusito,[53a,53b] G. Maggi,[53a,53c] M. Maggi,[53a]
B. Marangelli,[53a,53b] S. My,[53a,53c] S. Nuzzo,[53a,53b] N. Pacifico,[53a,53b] A. Pompili,[53a,53b] G. Pugliese,[53a,53c]
G. Selvaggi,[53a,53b] L. Silvestris,[53a] G. Singh,[53a,53b] R. Venditti,[53a,53b] G. Zito,[53a] G. Abbiendi,[54a] A. C. Benvenuti,[54a]
D. Bonacorsi,[54a,54b] S. Braibant-Giacomelli,[54a,54b] L. Brigliadori,[54a,54b] P. Capiluppi,[54a,54b] A. Castro,[54a,54b]
F. R. Cavallo,[54a] M. Cuffiani,[54a,54b] G. M. Dallavalle,[54a] F. Fabbri,[54a] A. Fanfani,[54a,54b] D. Fasanella,[54a,54b,f]
P. Giacomelli,[54a] C. Grandi,[54a] L. Guiducci,[54a,54b] S. Marcellini,[54a] G. Masetti,[54a] M. Meneghelli,[54a,54b,f]
A. Montanari,[54a] F. L. Navarria,[54a,54b] F. Odorici,[54a] A. Perrotta,[54a] F. Primavera,[54a,54b] A. M. Rossi,[54a,54b]
T. Rovelli,[54a,54b] G. Siroli,[54a,54b] R. Travaglini,[54a,54b] S. Albergo,[55a,55b] G. Cappello,[55a,55b] M. Chiorboli,[55a,55b]
S. Costa,[55a,55b] R. Potenza,[55a,55b] A. Tricomi,[55a,55b] C. Tuve,[55a,55b] G. Barbagli,[56a] V. Ciulli,[56a,56b] C. Civinini,[56a]
R. D'Alessandro,[56a,56b] E. Focardi,[56a,56b] S. Frosali,[56a,56b] E. Gallo,[56a] S. Gonzi,[56a,56b] M. Meschini,[56a] S. Paoletti,[56a]
G. Sguazzoni,[56a] A. Tropiano,[56a] L. Benussi,[57] S. Bianco,[57] S. Colafranceschi,[57,z] F. Fabbri,[57] D. Piccolo,[57]
P. Fabbricatore,[58a] R. Musenich,[58a] S. Tosi,[58a,58b] A. Benaglia,[59a,59b] F. De Guio,[59a,59b] L. Di Matteo,[59a,59b,f]
S. Fiorendi,[59a,59b] S. Gennai,[59a,f] A. Ghezzi,[59a,59b] S. Malvezzi,[59a] R. A. Manzoni,[59a,59b] A. Martelli,[59a,59b]
A. Massironi,[59a,59b,f] D. Menasce,[59a] L. Moroni,[59a] M. Paganoni,[59a,59b] D. Pedrini,[59a] S. Ragazzi,[59a,59b]
N. Redaelli,[59a] S. Sala,[59a] T. Tabarelli de Fatis,[59a,59b] S. Buontempo,[60a] C. A. Carrillo Montoya,[60a] N. Cavallo,[60a,aa]
A. De Cosa,[60a,60b,f] O. Dogangun,[60a,60b] F. Fabozzi,[60a,aa] A. O. M. Iorio,[60a] L. Lista,[60a] S. Meola,[60a,bb]
M. Merola,[60a,60b] P. Paolucci,[60a,f] P. Azzi,[61a] N. Bacchetta,[61a,f] D. Bisello,[61a,61b] A. Branca,[61a,61b,f] R. Carlin,[61a,61b]
P. Checchia,[61a] T. Dorigo,[61a] U. Dosselli,[61a] F. Gasparini,[61a,61b] U. Gasparini,[61a,61b] A. Gozzelino,[61a]
K. Kanishchev,[61a,61c] S. Lacaprara,[61a] I. Lazzizzera,[61a,61c] M. Margoni,[61a,61b] A. T. Meneguzzo,[61a,61b]
J. Pazzini,[61a,61b] N. Pozzobon,[61a,61b] P. Ronchese,[61a,61b] F. Simonetto,[61a,61b] E. Torassa,[61a] M. Tosi,[61a,61b,f]
S. Vanini,[61a,61b] P. Zotto,[61a,61b] G. Zumerle,[61a,61b] M. Gabusi,[62a,62b] S. P. Ratti,[62a,62b] C. Riccardi,[62a,62b]
P. Torre,[62a,62b] P. Vitulo,[62a,62b] M. Biasini,[63a,63b] G. M. Bilei,[63a] L. Fanò,[63a,63b] P. Lariccia,[63a,63b] A. Lucaroni,[63a,63b,f]
G. Mantovani,[63a,63b] M. Menichelli,[63a] A. Nappi,[63a,63b,a] F. Romeo,[63a,63b] A. Saha,[63a] A. Santocchia,[63a,63b]
A. Spiezia,[63a,63b] S. Taroni,[63a,63b] P. Azzurri,[64a,64c] G. Bagliesi,[64a] T. Boccali,[64a] G. Broccolo,[64a,64c] R. Castaldi,[64a]
R. T. D'Agnolo,[64a,64c,f] R. Dell'Orso,[64a] F. Fiori,[64a,64b,f] L. Foà,[64a,64c] A. Giassi,[64a] A. Kraan,[64a] F. Ligabue,[64a,64c]
T. Lomtadze,[64a] L. Martini,[64a,cc] A. Messineo,[64a,64b] F. Palla,[64a] A. Rizzi,[64a,64b] A. T. Serban,[64a,dd] P. Spagnolo,[64a]
P. Squillacioti,[64a,f] R. Tenchini,[64a] G. Tonelli,[64a,64b] A. Venturi,[64a] P. G. Verdini,[64a] L. Barone,[65a,65b] F. Cavallari,[65a]
D. Del Re,[65a,65b] M. Diemoz,[65a] C. Fanelli,[65a] M. Grassi,[65a,65b,f] E. Longo,[65a,65b] P. Meridiani,[65a,f] F. Micheli,[65a,65b]
S. Nourbakhsh,[65a,65b] G. Organtini,[65a,65b] R. Paramatti,[65a] S. Rahatlou,[65a,65b] M. Sigamani,[65a] L. Soffi,[65a,65b]
N. Amapane,[66a,66b] R. Arcidiacono,[66a,66c] S. Argiro,[66a,66b] M. Arneodo,[66a,66c] C. Biino,[66a] N. Cartiglia,[66a]
M. Costa,[66a,66b] P. De Remigis,[66a] N. Demaria,[66a] C. Mariotti,[66a,f] S. Maselli,[66a] E. Migliore,[66a,66b] V. Monaco,[66a,66b]
M. Musich,[66a,f] M. M. Obertino,[66a,66c] N. Pastrone,[66a] M. Pelliccioni,[66a] A. Potenza,[66a,66b] A. Romero,[66a,66b]
R. Sacchi,[66a,66b] A. Solano,[66a,66b] A. Staiano,[66a] A. Vilela Pereira,[66a] S. Belforte,[67a] V. Candelise,[67a,67b]
F. Cossutti,[67a] G. Della Ricca,[67a,67b] B. Gobbo,[67a] M. Marone,[67a,67b,f] D. Montanino,[67a,67b,f] A. Penzo,[67a]
A. Schizzi,[67a,67b] S. G. Heo,[68] T. Y. Kim,[68] S. K. Nam,[68] S. Chang,[69] D. H. Kim,[69] G. N. Kim,[69] D. J. Kong,[69]
H. Park,[69] S. R. Ro,[69] D. C. Son,[69] T. Son,[69] J. Y. Kim,[70] Zero J. Kim,[70] S. Song,[70] S. Choi,[71] D. Gyun,[71] B. Hong,[71]
M. Jo,[71] H. Kim,[71] T. J. Kim,[71] K. S. Lee,[71] D. H. Moon,[71] S. K. Park,[71] M. Choi,[72] J. H. Kim,[72] C. Park,[72]
I. C. Park,[72] S. Park,[72] G. Ryu,[72] Y. Cho,[73] Y. Choi,[73] Y. K. Choi,[73] J. Goh,[73] M. S. Kim,[73] E. Kwon,[73] B. Lee,[73]
J. Lee,[73] S. Lee,[73] H. Seo,[73] I. Yu,[73] M. J. Bilinskas,[74] I. Grigelionis,[74] M. Janulis,[74] A. Juodagalvis,[74]
H. Castilla-Valdez,[75] E. De La Cruz-Burelo,[75] I. Heredia-de La Cruz,[75] R. Lopez-Fernandez,[75] R. Magaña Villalba,[75]
J. Martínez-Ortega,[75] A. Sánchez-Hernández,[75] L. M. Villasenor-Cendejas,[75] S. Carrillo Moreno,[76]
F. Vazquez Valencia,[76] H. A. Salazar Ibarguen,[77] E. Casimiro Linares,[78] A. Morelos Pineda,[78] M. A. Reyes-Santos,[78]
D. Krofcheck,[79] A. J. Bell,[80] P. H. Butler,[80] R. Doesburg,[80] S. Reucroft,[80] H. Silverwood,[80] M. Ahmad,[81]
M. H. Ansari,[81] M. I. Asghar,[81] H. R. Hoorani,[81] S. Khalid,[81] W. A. Khan,[81] T. Khurshid,[81] S. Qazi,[81] M. A. Shah,[81]
M. Shoaib,[81] H. Bialkowska,[82] B. Boimska,[82] T. Frueboes,[82] R. Gokieli,[82] M. Górski,[82] M. Kazana,[82] K. Nawrocki,[82]

K. Romanowska-Rybinska,[82] M. Szleper,[82] G. Wrochna,[82] P. Zalewski,[82] G. Brona,[83] K. Bunkowski,[83] M. Cwiok,[83] W. Dominik,[83] K. Doroba,[83] A. Kalinowski,[83] M. Konecki,[83] J. Krolikowski,[83] N. Almeida,[84] P. Bargassa,[84] A. David,[84] P. Faccioli,[84] P. G. Ferreira Parracho,[84] M. Gallinaro,[84] J. Seixas,[84] J. Varela,[84] P. Vischia,[84] I. Belotelov,[85] P. Bunin,[85] I. Golutvin,[85] A. Kamenev,[85] V. Karjavin,[85] V. Konoplyanikov,[85] G. Kozlov,[85] A. Lanev,[85] A. Malakhov,[85] P. Moisenz,[85] V. Palichik,[85] V. Perelygin,[85] M. Savina,[85] S. Shmatov,[85] V. Smirnov,[85] A. Volodko,[85] A. Zarubin,[85] S. Evstyukhin,[86] V. Golovtsov,[86] Y. Ivanov,[86] V. Kim,[86] P. Levchenko,[86] V. Murzin,[86] V. Oreshkin,[86] I. Smirnov,[86] V. Sulimov,[86] L. Uvarov,[86] S. Vavilov,[86] A. Vorobyev,[86] An. Vorobyev,[86] Yu. Andreev,[87] A. Dermenev,[87] S. Gninenko,[87] N. Golubev,[87] M. Kirsanov,[87] N. Krasnikov,[87] V. Matveev,[87] A. Pashenkov,[87] D. Tlisov,[87] A. Toropin,[87] V. Epshteyn,[88] M. Erofeeva,[88] V. Gavrilov,[88] M. Kossov,[88] N. Lychkovskaya,[88] V. Popov,[88] G. Safronov,[88] S. Semenov,[88] V. Stolin,[88] E. Vlasov,[88] A. Zhokin,[88] A. Belyaev,[89] E. Boos,[89] M. Dubinin,[89,e] L. Dudko,[89] A. Ershov,[89] A. Gribushin,[89] V. Klyukhin,[89] O. Kodolova,[89] I. Lokhtin,[89] A. Markina,[89] S. Obraztsov,[89] M. Perfilov,[89] S. Petrushanko,[89] A. Popov,[89] L. Sarycheva,[89,a] V. Savrin,[89] A. Snigirev,[89] V. Andreev,[90] M. Azarkin,[90] I. Dremin,[90] M. Kirakosyan,[90] A. Leonidov,[90] G. Mesyats,[90] S. V. Rusakov,[90] A. Vinogradov,[90] I. Azhgirey,[91] I. Bayshev,[91] S. Bitioukov,[91] V. Grishin,[91,f] V. Kachanov,[91] D. Konstantinov,[91] V. Krychkine,[91] V. Petrov,[91] R. Ryutin,[91] A. Sobol,[91] L. Tourtchanovitch,[91] S. Troshin,[91] N. Tyurin,[91] A. Uzunian,[91] A. Volkov,[91] P. Adzic,[92,ee] M. Djordjevic,[92] M. Ekmedzic,[92] D. Krpic,[92,ee] J. Milosevic,[92] M. Aguilar-Benitez,[93] J. Alcaraz Maestre,[93] P. Arce,[93] C. Battilana,[93] E. Calvo,[93] M. Cerrada,[93] M. Chamizo Llatas,[93] N. Colino,[93] B. De La Cruz,[93] A. Delgado Peris,[93] D. Domínguez Vázquez,[93] C. Fernandez Bedoya,[93] J. P. Fernández Ramos,[93] A. Ferrando,[93] J. Flix,[93] M. C. Fouz,[93] P. Garcia-Abia,[93] O. Gonzalez Lopez,[93] S. Goy Lopez,[93] J. M. Hernandez,[93] M. I. Josa,[93] G. Merino,[93] J. Puerta Pelayo,[93] A. Quintario Olmeda,[93] I. Redondo,[93] L. Romero,[93] J. Santaolalla,[93] M. S. Soares,[93] C. Willmott,[93] C. Albajar,[94] G. Codispoti,[94] J. F. de Trocóniz,[94] H. Brun,[95] J. Cuevas,[95] J. Fernandez Menendez,[95] S. Folgueras,[95] I. Gonzalez Caballero,[95] L. Lloret Iglesias,[95] J. Piedra Gomez,[95] J. A. Brochero Cifuentes,[96] I. J. Cabrillo,[96] A. Calderon,[96] S. H. Chuang,[96] J. Duarte Campderros,[96] M. Felcini,[96,ff] M. Fernandez,[96] G. Gomez,[96] J. Gonzalez Sanchez,[96] A. Graziano,[96] C. Jorda,[96] A. Lopez Virto,[96] J. Marco,[96] R. Marco,[96] C. Martinez Rivero,[96] F. Matorras,[96] F. J. Munoz Sanchez,[96] T. Rodrigo,[96] A. Y. Rodríguez-Marrero,[96] A. Ruiz-Jimeno,[96] L. Scodellaro,[96] I. Vila,[96] R. Vilar Cortabitarte,[96] D. Abbaneo,[97] E. Auffray,[97] G. Auzinger,[97] M. Bachtis,[97] P. Baillon,[97] A. H. Ball,[97] D. Barney,[97] J. F. Benitez,[97] C. Bernet,[97,g] G. Bianchi,[97] P. Bloch,[97] A. Bocci,[97] A. Bonato,[97] C. Botta,[97] H. Breuker,[97] T. Camporesi,[97] G. Cerminara,[97] T. Christiansen,[97] J. A. Coarasa Perez,[97] D. D'Enterria,[97] A. Dabrowski,[97] A. De Roeck,[97] S. Di Guida,[97] M. Dobson,[97] N. Dupont-Sagorin,[97] A. Elliott-Peisert,[97] B. Frisch,[97] W. Funk,[97] G. Georgiou,[97] M. Giffels,[97] D. Gigi,[97] K. Gill,[97] D. Giordano,[97] M. Giunta,[97] F. Glege,[97] R. Gomez-Reino Garrido,[97] P. Govoni,[97] S. Gowdy,[97] R. Guida,[97] M. Hansen,[97] P. Harris,[97] C. Hartl,[97] J. Harvey,[97] B. Hegner,[97] A. Hinzmann,[97] V. Innocente,[97] P. Janot,[97] K. Kaadze,[97] E. Karavakis,[97] K. Kousouris,[97] P. Lecoq,[97] Y.-J. Lee,[97] P. Lenzi,[97] C. Lourenço,[97] N. Magini,[97] T. Mäki,[97] M. Malberti,[97] L. Malgeri,[97] M. Mannelli,[97] L. Masetti,[97] F. Meijers,[97] S. Mersi,[97] E. Meschi,[97] R. Moser,[97] M. U. Mozer,[97] M. Mulders,[97] P. Musella,[97] E. Nesvold,[97] T. Orimoto,[97] L. Orsini,[97] E. Palencia Cortezon,[97] E. Perez,[97] L. Perrozzi,[97] A. Petrilli,[97] A. Pfeiffer,[97] M. Pierini,[97] M. Pimiä,[97] D. Piparo,[97] G. Polese,[97] L. Quertenmont,[97] A. Racz,[97] W. Reece,[97] J. Rodrigues Antunes,[97] G. Rolandi,[97,gg] C. Rovelli,[97,hh] M. Rovere,[97] H. Sakulin,[97] F. Santanastasio,[97] C. Schäfer,[97] C. Schwick,[97] I. Segoni,[97] S. Sekmen,[97] A. Sharma,[97] P. Siegrist,[97] P. Silva,[97] M. Simon,[97] P. Sphicas,[97,ii] D. Spiga,[97] A. Tsirou,[97] G. I. Veres,[97,t] J. R. Vlimant,[97] H. K. Wöhri,[97] S. D. Worm,[97,jj] W. D. Zeuner,[97] W. Bertl,[98] K. Deiters,[98] W. Erdmann,[98] K. Gabathuler,[98] R. Horisberger,[98] Q. Ingram,[98] H. C. Kaestli,[98] S. König,[98] D. Kotlinski,[98] U. Langenegger,[98] F. Meier,[98] D. Renker,[98] T. Rohe,[98] J. Sibille,[98,kk] L. Bäni,[99] P. Bortignon,[99] M. A. Buchmann,[99] B. Casal,[99] N. Chanon,[99] A. Deisher,[99] G. Dissertori,[99] M. Dittmar,[99] M. Donegà,[99] M. Dünser,[99] J. Eugster,[99] K. Freudenreich,[99] C. Grab,[99] D. Hits,[99] P. Lecomte,[99] W. Lustermann,[99] A. C. Marini,[99] P. Martinez Ruiz del Arbol,[99] N. Mohr,[99] F. Moortgat,[99] C. Nägeli,[99,ll] P. Nef,[99] F. Nessi-Tedaldi,[99] F. Pandolfi,[99] L. Pape,[99] F. Pauss,[99] M. Peruzzi,[99] F. J. Ronga,[99] M. Rossini,[99] L. Sala,[99] A. K. Sanchez,[99] A. Starodumov,[99,mm] B. Stieger,[99] M. Takahashi,[99] L. Tauscher,[99,a] A. Thea,[99] K. Theofilatos,[99] D. Treille,[99] C. Urscheler,[99] R. Wallny,[99] H. A. Weber,[99] L. Wehrli,[99] C. Amsler,[100] V. Chiochia,[100] S. De Visscher,[100] C. Favaro,[100] M. Ivova Rikova,[100] B. Millan Mejias,[100] P. Otiougova,[100] P. Robmann,[100] H. Snoek,[100] S. Tupputi,[100] M. Verzetti,[100] Y. H. Chang,[101] K. H. Chen,[101] C. M. Kuo,[101] S. W. Li,[101] W. Lin,[101] Z. K. Liu,[101] Y. J. Lu,[101] D. Mekterovic,[101] A. P. Singh,[101] R. Volpe,[101] S. S. Yu,[101] P. Bartalini,[102] P. Chang,[102] Y. H. Chang,[102] Y. W. Chang,[102] Y. Chao,[102] K. F. Chen,[102] C. Dietz,[102] U. Grundler,[102] W.-S. Hou,[102] Y. Hsiung,[102] K. Y. Kao,[102] Y. J. Lei,[102] R.-S. Lu,[102] D. Majumder,[102]

E. Petrakou,[102] X. Shi,[102] J. G. Shiu,[102] Y. M. Tzeng,[102] X. Wan,[102] M. Wang,[102] A. Adiguzel,[103] M. N. Bakirci,[103,nn]
S. Cerci,[103,oo] C. Dozen,[103] I. Dumanoglu,[103] E. Eskut,[103] S. Girgis,[103] G. Gokbulut,[103] E. Gurpinar,[103] I. Hos,[103]
E. E. Kangal,[103] T. Karaman,[103] G. Karapinar,[103,pp] A. Kayis Topaksu,[103] G. Onengut,[103] K. Ozdemir,[103]
S. Ozturk,[103,qq] A. Polatoz,[103] K. Sogut,[103,rr] D. Sunar Cerci,[103,oo] B. Tali,[103,oo] H. Topakli,[103,nn] L. N. Vergili,[103]
M. Vergili,[103] I. V. Akin,[104] T. Aliev,[104] B. Bilin,[104] S. Bilmis,[104] M. Deniz,[104] H. Gamsizkan,[104] A. M. Guler,[104]
K. Ocalan,[104] A. Ozpineci,[104] M. Serin,[104] R. Sever,[104] U. E. Surat,[104] M. Yalvac,[104] E. Yildirim,[104] M. Zeyrek,[104]
E. Gülmez,[105] B. Isildak,[105,ss] M. Kaya,[105,tt] O. Kaya,[105,tt] S. Ozkorucuklu,[105,uu] N. Sonmez,[105,vv] K. Cankocak,[106]
L. Levchuk,[107] F. Bostock,[108] J. J. Brooke,[108] E. Clement,[108] D. Cussans,[108] H. Flacher,[108] R. Frazier,[108]
J. Goldstein,[108] M. Grimes,[108] G. P. Heath,[108] H. F. Heath,[108] L. Kreczko,[108] S. Metson,[108] D. M. Newbold,[108,jj]
K. Nirunpong,[108] A. Poll,[108] S. Senkin,[108] V. J. Smith,[108] T. Williams,[108] L. Basso,[109,ww] K. W. Bell,[109]
A. Belyaev,[109,ww] C. Brew,[109] R. M. Brown,[109] D. J. A. Cockerill,[109] J. A. Coughlan,[109] K. Harder,[109] S. Harper,[109]
J. Jackson,[109] B. W. Kennedy,[109] E. Olaiya,[109] D. Petyt,[109] B. C. Radburn-Smith,[109]
C. H. Shepherd-Themistocleous,[109] I. R. Tomalin,[109] W. J. Womersley,[109] R. Bainbridge,[110] G. Ball,[110]
R. Beuselinck,[110] O. Buchmuller,[110] D. Colling,[110] N. Cripps,[110] M. Cutajar,[110] P. Dauncey,[110] G. Davies,[110]
M. Della Negra,[110] W. Ferguson,[110] J. Fulcher,[110] D. Futyan,[110] A. Gilbert,[110] A. Guneratne Bryer,[110] G. Hall,[110]
Z. Hatherell,[110] J. Hays,[110] G. Iles,[110] M. Jarvis,[110] G. Karapostoli,[110] L. Lyons,[110] A.-M. Magnan,[110]
J. Marrouche,[110] B. Mathias,[110] R. Nandi,[110] J. Nash,[110] A. Nikitenko,[110,mm] A. Papageorgiou,[110] J. Pela,[110]
M. Pesaresi,[110] K. Petridis,[110] M. Pioppi,[110,xx] D. M. Raymond,[110] S. Rogerson,[110] A. Rose,[110] M. J. Ryan,[110]
C. Seez,[110] P. Sharp,[110,a] A. Sparrow,[110] M. Stoye,[110] A. Tapper,[110] M. Vazquez Acosta,[110] T. Virdee,[110]
S. Wakefield,[110] N. Wardle,[110] T. Whyntie,[110] M. Chadwick,[111] J. E. Cole,[111] P. R. Hobson,[111] A. Khan,[111]
P. Kyberd,[111] D. Leggat,[111] D. Leslie,[111] W. Martin,[111] I. D. Reid,[111] P. Symonds,[111] L. Teodorescu,[111] M. Turner,[111]
K. Hatakeyama,[112] H. Liu,[112] T. Scarborough,[112] O. Charaf,[113] C. Henderson,[113] P. Rumerio,[113] A. Avetisyan,[114]
T. Bose,[114] C. Fantasia,[114] A. Heister,[114] J. St. John,[114] P. Lawson,[114] D. Lazic,[114] J. Rohlf,[114] D. Sperka,[114]
L. Sulak,[114] J. Alimena,[115] S. Bhattacharya,[115] D. Cutts,[115] A. Ferapontov,[115] U. Heintz,[115] S. Jabeen,[115]
G. Kukartsev,[115] E. Laird,[115] G. Landsberg,[115] M. Luk,[115] M. Narain,[115] D. Nguyen,[115] M. Segala,[115]
T. Sinthuprasith,[115] T. Speer,[115] K. V. Tsang,[115] R. Breedon,[116] G. Breto,[116] M. Calderon De La Barca Sanchez,[116]
S. Chauhan,[116] M. Chertok,[116] J. Conway,[116] R. Conway,[116] P. T. Cox,[116] J. Dolen,[116] R. Erbacher,[116] M. Gardner,[116]
R. Houtz,[116] W. Ko,[116] A. Kopecky,[116] R. Lander,[116] T. Miceli,[116] D. Pellett,[116] F. Ricci-Tam,[116] B. Rutherford,[116]
M. Searle,[116] J. Smith,[116] M. Squires,[116] M. Tripathi,[116] R. Vasquez Sierra,[116] V. Andreev,[117] D. Cline,[117]
R. Cousins,[117] J. Duris,[117] S. Erhan,[117] P. Everaerts,[117] C. Farrell,[117] J. Hauser,[117] M. Ignatenko,[117] C. Jarvis,[117]
C. Plager,[117] G. Rakness,[117] P. Schlein,[117,a] P. Traczyk,[117] V. Valuev,[117] M. Weber,[117] J. Babb,[118] R. Clare,[118]
M. E. Dinardo,[118] J. Ellison,[118] J. W. Gary,[118] F. Giordano,[118] G. Hanson,[118] G. Y. Jeng,[118,yy] H. Liu,[118]
O. R. Long,[118] A. Luthra,[118] H. Nguyen,[118] S. Paramesvaran,[118] J. Sturdy,[118] S. Sumowidagdo,[118] R. Wilken,[118]
S. Wimpenny,[118] W. Andrews,[119] J. G. Branson,[119] G. B. Cerati,[119] S. Cittolin,[119] D. Evans,[119] F. Golf,[119]
A. Holzner,[119] R. Kelley,[119] M. Lebourgeois,[119] J. Letts,[119] I. Macneill,[119] B. Mangano,[119] S. Padhi,[119] C. Palmer,[119]
G. Petrucciani,[119] M. Pieri,[119] M. Sani,[119] V. Sharma,[119] S. Simon,[119] E. Sudano,[119] M. Tadel,[119] Y. Tu,[119]
A. Vartak,[119] S. Wasserbaech,[119,zz] F. Würthwein,[119] A. Yagil,[119] J. Yoo,[119] D. Barge,[120] R. Bellan,[120]
C. Campagnari,[120] M. D'Alfonso,[120] T. Danielson,[120] K. Flowers,[120] P. Geffert,[120] J. Incandela,[120] C. Justus,[120]
P. Kalavase,[120] S. A. Koay,[120] D. Kovalskyi,[120] V. Krutelyov,[120] S. Lowette,[120] N. Mccoll,[120] V. Pavlunin,[120]
F. Rebassoo,[120] J. Ribnik,[120] J. Richman,[120] R. Rossin,[120] D. Stuart,[120] W. To,[120] C. West,[120] A. Apresyan,[121]
A. Bornheim,[121] Y. Chen,[121] E. Di Marco,[121] J. Duarte,[121] M. Gataullin,[121] Y. Ma,[121] A. Mott,[121] H. B. Newman,[121]
C. Rogan,[121] M. Spiropulu,[121] V. Timciuc,[121] J. Veverka,[121] R. Wilkinson,[121] S. Xie,[121] Y. Yang,[121] R. Y. Zhu,[121]
B. Akgun,[122] V. Azzolini,[122] A. Calamba,[122] R. Carroll,[122] T. Ferguson,[122] Y. Iiyama,[122] D. W. Jang,[122] Y. F. Liu,[122]
M. Paulini,[122] H. Vogel,[122] I. Vorobiev,[122] J. P. Cumalat,[123] B. R. Drell,[123] C. J. Edelmaier,[123] W. T. Ford,[123]
A. Gaz,[123] B. Heyburn,[123] E. Luiggi Lopez,[123] J. G. Smith,[123] K. Stenson,[123] K. A. Ulmer,[123] S. R. Wagner,[123]
J. Alexander,[124] A. Chatterjee,[124] N. Eggert,[124] L. K. Gibbons,[124] B. Heltsley,[124] A. Khukhunaishvili,[124] B. Kreis,[124]
N. Mirman,[124] G. Nicolas Kaufman,[124] J. R. Patterson,[124] A. Ryd,[124] E. Salvati,[124] W. Sun,[124] W. D. Teo,[124]
J. Thom,[124] J. Thompson,[124] J. Tucker,[124] J. Vaughan,[124] Y. Weng,[124] L. Winstrom,[124] P. Wittich,[124] D. Winn,[125]
S. Abdullin,[126] M. Albrow,[126] J. Anderson,[126] L. A. T. Bauerdick,[126] A. Beretvas,[126] J. Berryhill,[126] P. C. Bhat,[126]
I. Bloch,[126] K. Burkett,[126] J. N. Butler,[126] V. Chetluru,[126] H. W. K. Cheung,[126] F. Chlebana,[126] V. D. Elvira,[126]
I. Fisk,[126] J. Freeman,[126] Y. Gao,[126] D. Green,[126] O. Gutsche,[126] J. Hanlon,[126] R. M. Harris,[126] J. Hirschauer,[126]

B. Hooberman,[126] S. Jindariani,[126] M. Johnson,[126] U. Joshi,[126] B. Kilminster,[126] B. Klima,[126] S. Kunori,[126]
S. Kwan,[126] C. Leonidopoulos,[126] J. Linacre,[126] D. Lincoln,[126] R. Lipton,[126] J. Lykken,[126] K. Maeshima,[126]
J. M. Marraffino,[126] S. Maruyama,[126] D. Mason,[126] P. McBride,[126] K. Mishra,[126] S. Mrenna,[126] Y. Musienko,[126,aaa]
C. Newman-Holmes,[126] V. O'Dell,[126] O. Prokofyev,[126] E. Sexton-Kennedy,[126] S. Sharma,[126] W. J. Spalding,[126]
L. Spiegel,[126] P. Tan,[126] L. Taylor,[126] S. Tkaczyk,[126] N. V. Tran,[126] L. Uplegger,[126] E. W. Vaandering,[126] R. Vidal,[126]
J. Whitmore,[126] W. Wu,[126] F. Yang,[126] F. Yumiceva,[126] J. C. Yun,[126] D. Acosta,[127] P. Avery,[127] D. Bourilkov,[127]
M. Chen,[127] T. Cheng,[127] S. Das,[127] M. De Gruttola,[127] G. P. Di Giovanni,[127] D. Dobur,[127] A. Drozdetskiy,[127]
R. D. Field,[127] M. Fisher,[127] Y. Fu,[127] I. K. Furic,[127] J. Gartner,[127] J. Hugon,[127] B. Kim,[127] J. Konigsberg,[127]
A. Korytov,[127] A. Kropivnitskaya,[127] T. Kypreos,[127] J. F. Low,[127] K. Matchev,[127] P. Milenovic,[127,bbb]
G. Mitselmakher,[127] L. Muniz,[127] M. Park,[127] R. Remington,[127] A. Rinkevicius,[127] P. Sellers,[127] N. Skhirtladze,[127]
M. Snowball,[127] J. Yelton,[127] M. Zakaria,[127] V. Gaultney,[128] S. Hewamanage,[128] L. M. Lebolo,[128] S. Linn,[128]
P. Markowitz,[128] G. Martinez,[128] J. L. Rodriguez,[128] T. Adams,[129] A. Askew,[129] J. Bochenek,[129] J. Chen,[129]
B. Diamond,[129] S. V. Gleyzer,[129] J. Haas,[129] S. Hagopian,[129] V. Hagopian,[129] M. Jenkins,[129] K. F. Johnson,[129]
H. Prosper,[129] V. Veeraraghavan,[129] M. Weinberg,[129] M. M. Baarmand,[130] B. Dorney,[130] M. Hohlmann,[130]
H. Kalakhety,[130] I. Vodopiyanov,[130] M. R. Adams,[131] I. M. Anghel,[131] L. Apanasevich,[131] Y. Bai,[131]
V. E. Bazterra,[131] R. R. Betts,[131] I. Bucinskaite,[131] J. Callner,[131] R. Cavanaugh,[131] O. Evdokimov,[131] L. Gauthier,[131]
C. E. Gerber,[131] D. J. Hofman,[131] S. Khalatyan,[131] F. Lacroix,[131] M. Malek,[131] C. O'Brien,[131] C. Silkworth,[131]
D. Strom,[131] P. Turner,[131] N. Varelas,[131] U. Akgun,[132] E. A. Albayrak,[132] B. Bilki,[132,ccc] W. Clarida,[132] F. Duru,[132]
S. Griffiths,[132] J.-P. Merlo,[132] H. Mermerkaya,[132,ddd] A. Mestvirishvili,[132] A. Moeller,[132] J. Nachtman,[132]
C. R. Newsom,[132] E. Norbeck,[132] Y. Onel,[132] F. Ozok,[132] S. Sen,[132] E. Tiras,[132] J. Wetzel,[132] T. Yetkin,[132] K. Yi,[132]
B. A. Barnett,[133] B. Blumenfeld,[133] S. Bolognesi,[133] D. Fehling,[133] G. Giurgiu,[133] A. V. Gritsan,[133] Z. J. Guo,[133]
G. Hu,[133] P. Maksimovic,[133] S. Rappoccio,[133] M. Swartz,[133] A. Whitbeck,[133] P. Baringer,[134] A. Bean,[134]
G. Benelli,[134] R. P. Kenny Iii,[134] M. Murray,[134] D. Noonan,[134] S. Sanders,[134] R. Stringer,[134] G. Tinti,[134]
J. S. Wood,[134] V. Zhukova,[134] A. F. Barfuss,[135] T. Bolton,[135] I. Chakaberia,[135] A. Ivanov,[135] S. Khalil,[135]
M. Makouski,[135] Y. Maravin,[135] S. Shrestha,[135] I. Svintradze,[135] J. Gronberg,[136] D. Lange,[136] D. Wright,[136]
A. Baden,[137] M. Boutemeur,[137] B. Calvert,[137] S. C. Eno,[137] J. A. Gomez,[137] N. J. Hadley,[137] R. G. Kellogg,[137]
M. Kirn,[137] T. Kolberg,[137] Y. Lu,[137] M. Marionneau,[137] A. C. Mignerey,[137] K. Pedro,[137] A. Peterman,[137] A. Skuja,[137]
J. Temple,[137] M. B. Tonjes,[137] S. C. Tonwar,[137] E. Twedt,[137] A. Apyan,[138] G. Bauer,[138] J. Bendavid,[138] W. Busza,[138]
E. Butz,[138] I. A. Cali,[138] M. Chan,[138] V. Dutta,[138] G. Gomez Ceballos,[138] M. Goncharov,[138] K. A. Hahn,[138]
Y. Kim,[138] M. Klute,[138] K. Krajczar,[138,eee] W. Li,[138] P. D. Luckey,[138] T. Ma,[138] S. Nahn,[138] C. Paus,[138] D. Ralph,[138]
C. Roland,[138] G. Roland,[138] M. Rudolph,[138] G. S. F. Stephans,[138] F. Stöckli,[138] K. Sumorok,[138] K. Sung,[138]
D. Velicanu,[138] E. A. Wenger,[138] R. Wolf,[138] B. Wyslouch,[138] M. Yang,[138] Y. Yilmaz,[138] A. S. Yoon,[138] M. Zanetti,[138]
S. I. Cooper,[139] B. Dahmes,[139] A. De Benedetti,[139] G. Franzoni,[139] A. Gude,[139] S. C. Kao,[139] K. Klapoetke,[139]
Y. Kubota,[139] J. Mans,[139] N. Pastika,[139] R. Rusack,[139] M. Sasseville,[139] A. Singovsky,[139] N. Tambe,[139]
J. Turkewitz,[139] L. M. Cremaldi,[140] R. Kroeger,[140] L. Perera,[140] R. Rahmat,[140] D. A. Sanders,[140] E. Avdeeva,[141]
K. Bloom,[141] S. Bose,[141] J. Butt,[141] D. R. Claes,[141] A. Dominguez,[141] M. Eads,[141] J. Keller,[141] I. Kravchenko,[141]
J. Lazo-Flores,[141] H. Malbouisson,[141] S. Malik,[141] G. R. Snow,[141] U. Baur,[142] A. Godshalk,[142] I. Iashvili,[142]
S. Jain,[142] A. Kharchilava,[142] A. Kumar,[142] S. P. Shipkowski,[142] K. Smith,[142] G. Alverson,[143] E. Barberis,[143]
D. Baumgartel,[143] M. Chasco,[143] J. Haley,[143] D. Nash,[143] D. Trocino,[143] D. Wood,[143] J. Zhang,[143] A. Anastassov,[144]
A. Kubik,[144] N. Mucia,[144] N. Odell,[144] R. A. Ofierzynski,[144] B. Pollack,[144] A. Pozdnyakov,[144] M. Schmitt,[144]
S. Stoynev,[144] M. Velasco,[144] S. Won,[144] L. Antonelli,[145] D. Berry,[145] A. Brinkerhoff,[145] M. Hildreth,[145]
C. Jessop,[145] D. J. Karmgard,[145] J. Kolb,[145] K. Lannon,[145] W. Luo,[145] S. Lynch,[145] N. Marinelli,[145] D. M. Morse,[145]
T. Pearson,[145] M. Planer,[145] R. Ruchti,[145] J. Slaunwhite,[145] N. Valls,[145] M. Wayne,[145] M. Wolf,[145] B. Bylsma,[146]
L. S. Durkin,[146] C. Hill,[146] R. Hughes,[146] K. Kotov,[146] T. Y. Ling,[146] D. Puigh,[146] M. Rodenburg,[146] C. Vuosalo,[146]
G. Williams,[146] B. L. Winer,[146] N. Adam,[147] E. Berry,[147] P. Elmer,[147] D. Gerbaudo,[147] V. Halyo,[147] P. Hebda,[147]
J. Hegeman,[147] A. Hunt,[147] P. Jindal,[147] D. Lopes Pegna,[147] P. Lujan,[147] D. Marlow,[147] T. Medvedeva,[147]
M. Mooney,[147] J. Olsen,[147] P. Piroué,[147] X. Quan,[147] A. Raval,[147] B. Safdi,[147] H. Saka,[147] D. Stickland,[147]
C. Tully,[147] J. S. Werner,[147] A. Zuranski,[147] J. G. Acosta,[148] E. Brownson,[148] X. T. Huang,[148] A. Lopez,[148]
H. Mendez,[148] S. Oliveros,[148] J. E. Ramirez Vargas,[148] A. Zatserklyaniy,[148] E. Alagoz,[149] V. E. Barnes,[149]
D. Benedetti,[149] G. Bolla,[149] D. Bortoletto,[149] M. De Mattia,[149] A. Everett,[149] Z. Hu,[149] M. Jones,[149] O. Koybasi,[149]
M. Kress,[149] A. T. Laasanen,[149] N. Leonardo,[149] V. Maroussov,[149] P. Merkel,[149] D. H. Miller,[149] N. Neumeister,[149]

I. Shipsey,[149] D. Silvers,[149] A. Svyatkovskiy,[149] M. Vidal Marono,[149] H. D. Yoo,[149] J. Zablocki,[149] Y. Zheng,[149]
S. Guragain,[150] N. Parashar,[150] A. Adair,[151] C. Boulahouache,[151] K. M. Ecklund,[151] F. J. M. Geurts,[151]
B. P. Padley,[151] R. Redjimi,[151] J. Roberts,[151] J. Zabel,[151] B. Betchart,[152] A. Bodek,[152] Y. S. Chung,[152] R. Covarelli,[152]
P. de Barbaro,[152] R. Demina,[152] Y. Eshaq,[152] T. Ferbel,[152] A. Garcia-Bellido,[152] P. Goldenzweig,[152] J. Han,[152]
A. Harel,[152] D. C. Miner,[152] D. Vishnevskiy,[152] M. Zielinski,[152] A. Bhatti,[153] R. Ciesielski,[153] L. Demortier,[153]
K. Goulianos,[153] G. Lungu,[153] S. Malik,[153] C. Mesropian,[153] S. Arora,[154] A. Barker,[154] J. P. Chou,[154]
C. Contreras-Campana,[154] E. Contreras-Campana,[154] D. Duggan,[154] D. Ferencek,[154] Y. Gershtein,[154] R. Gray,[154]
E. Halkiadakis,[154] D. Hidas,[154] A. Lath,[154] S. Panwalkar,[154] M. Park,[154] R. Patel,[154] V. Rekovic,[154] J. Robles,[154]
K. Rose,[154] S. Salur,[154] S. Schnetzer,[154] C. Seitz,[154] S. Somalwar,[154] R. Stone,[154] S. Thomas,[154] G. Cerizza,[155]
M. Hollingsworth,[155] S. Spanier,[155] Z. C. Yang,[155] A. York,[155] R. Eusebi,[156] W. Flanagan,[156] J. Gilmore,[156]
T. Kamon,[156,fff] V. Khotilovich,[156] R. Montalvo,[156] I. Osipenkov,[156] Y. Pakhotin,[156] A. Perloff,[156] J. Roe,[156]
A. Safonov,[156] T. Sakuma,[156] S. Sengupta,[156] I. Suarez,[156] A. Tatarinov,[156] D. Toback,[156] N. Akchurin,[157]
J. Damgov,[157] C. Dragoiu,[157] P. R. Dudero,[157] C. Jeong,[157] K. Kovitanggoon,[157] S. W. Lee,[157] T. Libeiro,[157]
Y. Roh,[157] I. Volobouev,[157] E. Appelt,[158] A. G. Delannoy,[158] C. Florez,[158] S. Greene,[158] A. Gurrola,[158] W. Johns,[158]
C. Johnston,[158] P. Kurt,[158] C. Maguire,[158] A. Melo,[158] M. Sharma,[158] P. Sheldon,[158] B. Snook,[158] S. Tuo,[158]
J. Velkovska,[158] M. W. Arenton,[159] M. Balazs,[159] S. Boutle,[159] B. Cox,[159] B. Francis,[159] J. Goodell,[159] R. Hirosky,[159]
A. Ledovskoy,[159] C. Lin,[159] C. Neu,[159] J. Wood,[159] R. Yohay,[159] S. Gollapinni,[160] R. Harr,[160] P. E. Karchin,[160]
C. Kottachchi Kankanamge Don,[160] P. Lamichhane,[160] A. Sakharov,[160] M. Anderson,[161] D. Belknap,[161]
L. Borrello,[161] D. Carlsmith,[161] M. Cepeda,[161] S. Dasu,[161] E. Friis,[161] L. Gray,[161] K. S. Grogg,[161] M. Grothe,[161]
R. Hall-Wilton,[161] M. Herndon,[161] A. Hervé,[161] P. Klabbers,[161] J. Klukas,[161] A. Lanaro,[161] C. Lazaridis,[161]
J. Leonard,[161] R. Loveless,[161] A. Mohapatra,[161] I. Ojalvo,[161] F. Palmonari,[161] G. A. Pierro,[161] I. Ross,[161] A. Savin,[161]
W. H. Smith,[161] and J. Swanson[161]

(CMS Collaboration)

[1]*Yerevan Physics Institute, Yerevan, Armenia*
[2]*Institut für Hochenergiephysik der OeAW, Wien, Austria*
[3]*National Centre for Particle and High Energy Physics, Minsk, Belarus*
[4]*Universiteit Antwerpen, Antwerpen, Belgium*
[5]*Vrije Universiteit Brussel, Brussel, Belgium*
[6]*Université Libre de Bruxelles, Bruxelles, Belgium*
[7]*Ghent University, Ghent, Belgium*
[8]*Université Catholique de Louvain, Louvain-la-Neuve, Belgium*
[9]*Université de Mons, Mons, Belgium*
[10]*Centro Brasileiro de Pesquisas Fisicas, Rio de Janeiro, Brazil*
[11]*Universidade do Estado do Rio de Janeiro, Rio de Janeiro, Brazil*
[12]*Instituto de Fisica Teorica, Universidade Estadual Paulista, Sao Paulo, Brazil*
[13]*Institute for Nuclear Research and Nuclear Energy, Sofia, Bulgaria*
[14]*University of Sofia, Sofia, Bulgaria*
[15]*Institute of High Energy Physics, Beijing, China*
[16]*State Key Laboratory of Nuclear Physics and Technology, Peking University, Beijing, China*
[17]*Universidad de Los Andes, Bogota, Colombia*
[18]*Technical University of Split, Split, Croatia*
[19]*University of Split, Split, Croatia*
[20]*Institute Rudjer Boskovic, Zagreb, Croatia*
[21]*University of Cyprus, Nicosia, Cyprus*
[22]*Charles University, Prague, Czech Republic*
[23]*Academy of Scientific Research and Technology of the Arab Republic of Egypt,
Egyptian Network of High Energy Physics, Cairo, Egypt*
[24]*National Institute of Chemical Physics and Biophysics, Tallinn, Estonia*
[25]*Department of Physics, University of Helsinki, Helsinki, Finland*
[26]*Helsinki Institute of Physics, Helsinki, Finland*
[27]*Lappeenranta University of Technology, Lappeenranta, Finland*
[28]*DSM/IRFU, CEA/Saclay, Gif-sur-Yvette, France*
[29]*Laboratoire Leprince-Ringuet, Ecole Polytechnique, IN2P3-CNRS, Palaiseau, France*

[30]*Institut Pluridisciplinaire Hubert Curien, Université de Strasbourg, Université de Haute Alsace Mulhouse, CNRS/IN2P3, Strasbourg, France*

[31]*Centre de Calcul de l'Institut National de Physique Nucleaire et de Physique des Particules, CNRS/IN2P3, Villeurbanne, France*

[32]*Université de Lyon, Université Claude Bernard Lyon 1, CNRS-IN2P3, Institut de Physique Nucléaire de Lyon, Villeurbanne, France*

[33]*Institute of High Energy Physics and Informatization, Tbilisi State University, Tbilisi, Georgia*

[34]*RWTH Aachen University, I. Physikalisches Institut, Aachen, Germany*

[35]*RWTH Aachen University, III. Physikalisches Institut A, Aachen, Germany*

[36]*RWTH Aachen University, III. Physikalisches Institut B, Aachen, Germany*

[37]*Deutsches Elektronen-Synchrotron, Hamburg, Germany*

[38]*University of Hamburg, Hamburg, Germany*

[39]*Institut für Experimentelle Kernphysik, Karlsruhe, Germany*

[40]*Institute of Nuclear Physics "Demokritos", Aghia Paraskevi, Greece*

[41]*University of Athens, Athens, Greece*

[42]*University of Ioánnina, Ioánnina, Greece*

[43]*KFKI Research Institute for Particle and Nuclear Physics, Budapest, Hungary*

[44]*Institute of Nuclear Research ATOMKI, Debrecen, Hungary*

[45]*University of Debrecen, Debrecen, Hungary*

[46]*Panjab University, Chandigarh, India*

[47]*University of Delhi, Delhi, India*

[48]*Saha Institute of Nuclear Physics, Kolkata, India*

[49]*Bhabha Atomic Research Centre, Mumbai, India*

[50]*Tata Institute of Fundamental Research-EHEP, Mumbai, India*

[51]*Tata Institute of Fundamental Research-HECR, Mumbai, India*

[52]*Institute for Research in Fundamental Sciences (IPM), Tehran, Iran*

[53a]*INFN Sezione di Bari, Bari, Italy*

[53b]*Università di Bari, Bari, Italy*

[53c]*Politecnico di Bari, Bari, Italy*

[54a]*INFN Sezione di Bologna, Bologna, Italy*

[54b]*Università di Bologna, Bologna, Italy*

[55a]*INFN Sezione di Catania, Catania, Italy*

[55b]*Università di Catania, Catania, Italy*

[56a]*INFN Sezione di Firenze, Firenze, Italy*

[56b]*Università di Firenze, Firenze, Italy*

[57]*INFN Laboratori Nazionali di Frascati, Frascati, Italy*

[58a]*INFN Sezione di Genova, Genova, Italy*

[58b]*Università di Genova, Genova, Italy*

[59a]*INFN Sezione di Milano-Bicocca, Milano, Italy*

[59b]*Università di Milano-Bicocca, Milano, Italy*

[60a]*INFN Sezione di Napoli, Napoli, Italy*

[60b]*Università di Napoli "Federico II", Napoli, Italy*

[61a]*INFN Sezione di Padova, Padova, Italy*

[61b]*Università di Padova, Padova, Italy*

[61c]*Università di Trento (Trento), Padova, Italy*

[62a]*INFN Sezione di Pavia, Pavia, Italy*

[62b]*Università di Pavia, Pavia, Italy*

[63a]*INFN Sezione di Perugia, Perugia, Italy*

[63b]*Università di Perugia, Perugia, Italy*

[64a]*INFN Sezione di Pisa, Pisa, Italy*

[64b]*Università di Pisa, Pisa, Italy*

[64c]*Scuola Normale Superiore di Pisa, Pisa, Italy*

[65a]*INFN Sezione di Roma, Roma, Italy*

[65b]*Università di Roma "La Sapienza", Roma, Italy*

[66a]*INFN Sezione di Torino, Torino, Italy*

[66b]*Università di Torino, Torino, Italy*

[66c]*Università del Piemonte Orientale (Novara), Torino, Italy*

[67a]*INFN Sezione di Trieste, Trieste, Italy*

[67b]*Università di Trieste, Trieste, Italy*

[68]*Kangwon National University, Chunchon, Korea*

[69]*Kyungpook National University, Daegu, Korea*

[70]*Chonnam National University, Institute for Universe and Elementary Particles, Kwangju, Korea*

[71]*Korea University, Seoul, Korea*

[72]University of Seoul, Seoul, Korea
[73]Sungkyunkwan University, Suwon, Korea
[74]Vilnius University, Vilnius, Lithuania
[75]Centro de Investigacion y de Estudios Avanzados del IPN, Mexico City, Mexico
[76]Universidad Iberoamericana, Mexico City, Mexico
[77]Benemerita Universidad Autonoma de Puebla, Puebla, Mexico
[78]Universidad Autónoma de San Luis Potosí, San Luis Potosí, Mexico
[79]University of Auckland, Auckland, New Zealand
[80]University of Canterbury, Christchurch, New Zealand
[81]National Centre for Physics, Quaid-I-Azam University, Islamabad, Pakistan
[82]National Centre for Nuclear Research, Swierk, Poland
[83]Institute of Experimental Physics, Faculty of Physics, University of Warsaw, Warsaw, Poland
[84]Laboratório de Instrumentação e Física Experimental de Partículas, Lisboa, Portugal
[85]Joint Institute for Nuclear Research, Dubna, Russia
[86]Petersburg Nuclear Physics Institute, Gatchina (St Petersburg), Russia
[87]Institute for Nuclear Research, Moscow, Russia
[88]Institute for Theoretical and Experimental Physics, Moscow, Russia
[89]Moscow State University, Moscow, Russia
[90]P. N. Lebedev Physical Institute, Moscow, Russia
[91]State Research Center of Russian Federation, Institute for High Energy Physics, Protvino, Russia
[92]University of Belgrade, Faculty of Physics and Vinca Institute of Nuclear Sciences, Belgrade, Serbia
[93]Centro de Investigaciones Energéticas Medioambientales y Tecnológicas (CIEMAT), Madrid, Spain
[94]Universidad Autónoma de Madrid, Madrid, Spain
[95]Universidad de Oviedo, Oviedo, Spain
[96]Instituto de Física de Cantabria (IFCA), CSIC-Universidad de Cantabria, Santander, Spain
[97]CERN, European Organization for Nuclear Research, Geneva, Switzerland
[98]Paul Scherrer Institut, Villigen, Switzerland
[99]Institute for Particle Physics, ETH Zurich, Zurich, Switzerland
[100]Universität Zürich, Zurich, Switzerland
[101]National Central University, Chung-Li, Taiwan
[102]National Taiwan University (NTU), Taipei, Taiwan
[103]Cukurova University, Adana, Turkey
[104]Middle East Technical University, Physics Department, Ankara, Turkey
[105]Bogazici University, Istanbul, Turkey
[106]Istanbul Technical University, Istanbul, Turkey
[107]National Scientific Center, Kharkov Institute of Physics and Technology, Kharkov, Ukraine
[108]University of Bristol, Bristol, United Kingdom
[109]Rutherford Appleton Laboratory, Didcot, United Kingdom
[110]Imperial College, London, United Kingdom
[111]Brunel University, Uxbridge, United Kingdom
[112]Baylor University, Waco, USA
[113]The University of Alabama, Tuscaloosa, Alabama, USA
[114]Boston University, Boston, Massachusetts, USA
[115]Brown University, Providence, Rhode Island, USA
[116]University of California, Davis, California, USA
[117]University of California, Los Angeles, Los Angeles, California, USA
[118]University of California, Riverside, Riverside, California, USA
[119]University of California, San Diego, La Jolla, California, USA
[120]University of California, Santa Barbara, Santa Barbara, California, USA
[121]California Institute of Technology, Pasadena, California, USA
[122]Carnegie Mellon University, Pittsburgh, Pennsylvania, USA
[123]University of Colorado at Boulder, Boulder, Colorado, USA
[124]Cornell University, Ithaca, New York, USA
[125]Fairfield University, Fairfield, Connecticut, USA
[126]Fermi National Accelerator Laboratory, Batavia, Illinois, USA
[127]University of Florida, Gainesville, Florida, USA
[128]Florida International University, Miami, Florida, USA
[129]Florida State University, Tallahassee, Florida, USA
[130]Florida Institute of Technology, Melbourne, Florida, USA
[131]University of Illinois at Chicago (UIC), Chicago, Illinois, USA
[132]The University of Iowa, Iowa City, Iowa, USA

[133] *Johns Hopkins University, Baltimore, Maryland, USA*

[134] *The University of Kansas, Lawrence, Kansas, USA*

[135] *Kansas State University, Manhattan, Kansas, USA*

[136] *Lawrence Livermore National Laboratory, Livermore, California, USA*

[137] *University of Maryland, College Park, Maryland, USA*

[138] *Massachusetts Institute of Technology, Cambridge, Massachusetts, USA*

[139] *University of Minnesota, Minneapolis, Minnesota, USA*

[140] *University of Mississippi, University, Mississippi, USA*

[141] *University of Nebraska-Lincoln, Lincoln, Nebraska, USA*

[142] *State University of New York at Buffalo, Buffalo, New York, USA*

[143] *Northeastern University, Boston, Massachusetts, USA*

[144] *Northwestern University, Evanston, Illinois, USA*

[145] *University of Notre Dame, Notre Dame, Indiana, USA*

[146] *The Ohio State University, Columbus, Ohio, USA*

[147] *Princeton University, Princeton, New Jersey, USA*

[148] *University of Puerto Rico, Mayaguez, Puerto Rico*

[149] *Purdue University, West Lafayette, Indiana, USA*

[150] *Purdue University Calumet, Hammond, Indiana, USA*

[151] *Rice University, Houston, Texas, USA*

[152] *University of Rochester, Rochester, New York, USA*

[153] *The Rockefeller University, New York, New York, USA*

[154] *Rutgers, the State University of New Jersey, Piscataway, New Jersey, USA*

[155] *University of Tennessee, Knoxville, Tennessee, USA*

[156] *Texas A&M University, College Station, Texas, USA*

[157] *Texas Tech University, Lubbock, Texas, USA*

[158] *Vanderbilt University, Nashville, Tennessee, USA*

[159] *University of Virginia, Charlottesville, Virginia, USA*

[160] *Wayne State University, Detroit, Michigan, USA*

[161] *University of Wisconsin, Madison, Wisconsin, USA*

[a] Deceased.

[b] Also at Vienna University of Technology, Vienna, Austria

[c] Also at National Institute of Chemical Physics and Biophysics, Tallinn, Estonia

[d] Also at Universidade Federal do ABC, Santo Andre, Brazil

[e] Also at California Institute of Technology, Pasadena, California, USA

[f] Also at CERN, European Organization for Nuclear Research, Geneva, Switzerland

[g] Also at Laboratoire Leprince-Ringuet, Ecole Polytechnique, IN2P3-CNRS, Palaiseau, France

[h] Also at Suez Canal University, Suez, Egypt

[i] Also at Zewail City of Science and Technology, Zewail, Egypt

[j] Also at Cairo University, Cairo, Egypt

[k] Also at Fayoum University, El-Fayoum, Egypt

[l] Also at British University, Cairo, Egypt

[m] Now at Ain Shams University, Cairo, Egypt

[n] Also at National Centre for Nuclear Research, Swierk, Poland

[o] Also at Université de Haute-Alsace, Mulhouse, France

[p] Now at Joint Institute for Nuclear Research, Dubna, Russia

[q] Also at Moscow State University, Moscow, Russia

[r] Also at Brandenburg University of Technology, Cottbus, Germany

[s] Also at Institute of Nuclear Research ATOMKI, Debrecen, Hungary

[t] Also at Eötvös Loránd University, Budapest, Hungary

[u] Also at Tata Institute of Fundamental Research-HECR, Mumbai, India

[v] Also at University of Visva-Bharati, Santiniketan, India

[w] Also at Sharif University of Technology, Tehran, Iran

[x] Also at Isfahan University of Technology, Isfahan, Iran

[y] Also at Plasma Physics Research Center, Science and Research Branch, Islamic Azad University, Teheran, Iran

[z] Also at Facoltà Ingegneria Università di Roma, Roma, Italy

[aa] Also at Università della Basilicata, Potenza, Italy

[bb] Also at Università degli Studi Guglielmo Marconi, Roma, Italy

[cc]Also at Università degli Studi di Siena, Siena, Italy

[dd]Also at University of Bucharest, Faculty of Physics, Bucuresti-Magurele, Romania

[ee]Also at Faculty of Physics of University of Belgrade, Belgrade, Serbia

[ff]Also at University of California, Los Angeles, Los Angeles, California, USA

[gg]Also at Scuola Normale e Sezione dell' INFN, Pisa, Italy

[hh]Also at INFN Sezione di Roma, Università di Roma ''La Sapienza,'' Roma, Italy

[ii]Also at University of Athens, Athens, Greece

[jj]Also at Rutherford Appleton Laboratory, Didcot, United Kingdom

[kk]Also at The University of Kansas, Lawrence, Kansas, USA

[ll]Also at Paul Scherrer Institut, Villigen, Switzerland

[mm]Also at Institute for Theoretical and Experimental Physics, Moscow, Russia

[nn]Also at Gaziosmanpasa University, Tokat, Turkey

[oo]Also at Adiyaman University, Adiyaman, Turkey

[pp]Also at Izmir Institute of Technology, Izmir, Turkey

[qq]Also at The University of Iowa, Iowa City, Iowa, USA

[rr]Also at Mersin University, Mersin, Turkey

[ss]Also at Ozyegin University, Istanbul, Turkey

[tt]Also at Kafkas University, Kars, Turkey

[uu]Also at Suleyman Demirel University, Isparta, Turkey

[vv]Also at Ege University, Izmir, Turkey

[ww]Also at School of Physics and Astronomy, University of Southampton, Southampton, United Kingdom

[xx]Also at INFN Sezione di Perugia, Università di Perugia, Perugia, Italy

[yy]Also at University of Sydney, Sydney, Australia

[zz]Also at Utah Valley University, Orem, Utah, USA

[aaa]Also at Institute for Nuclear Research, Moscow, Russia

[bbb]Also at University of Belgrade, Faculty of Physics and Vinca Institute of Nuclear Sciences, Belgrade, Serbia

[ccc]Also at Argonne National Laboratory, Argonne, Illinois, USA

[ddd]Also at Erzincan University, Erzincan, Turkey

[eee]Also at KFKI Research Institute for Particle and Nuclear Physics, Budapest, Hungary

[fff]Also at Kyungpook National University, Daegu, Korea